Computational Bioengineering Overview of Modeling Activities

Philippe Büchler

ARTORG Center for Biomedical Engineering Research
University of Bern, Switzerland

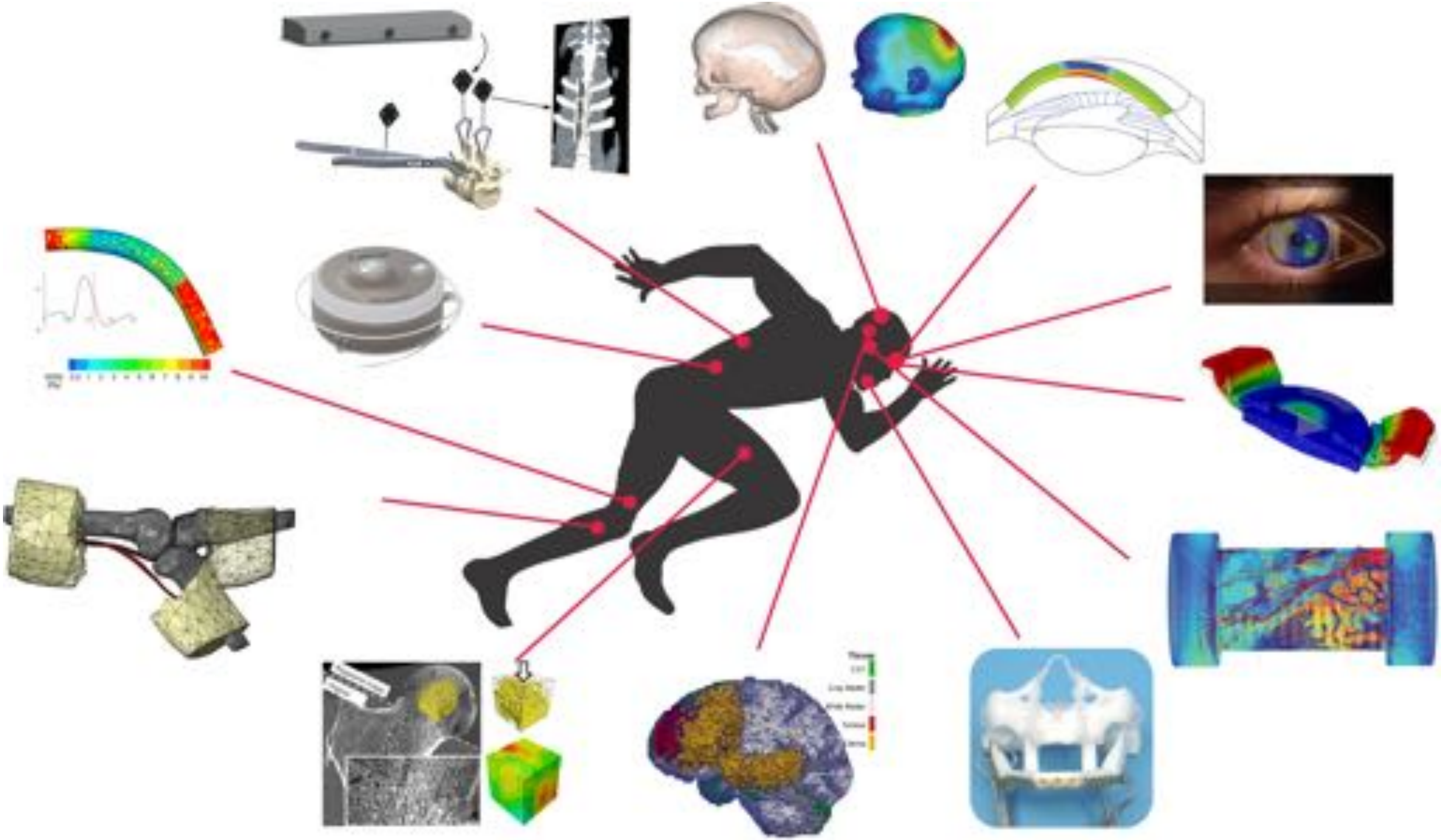

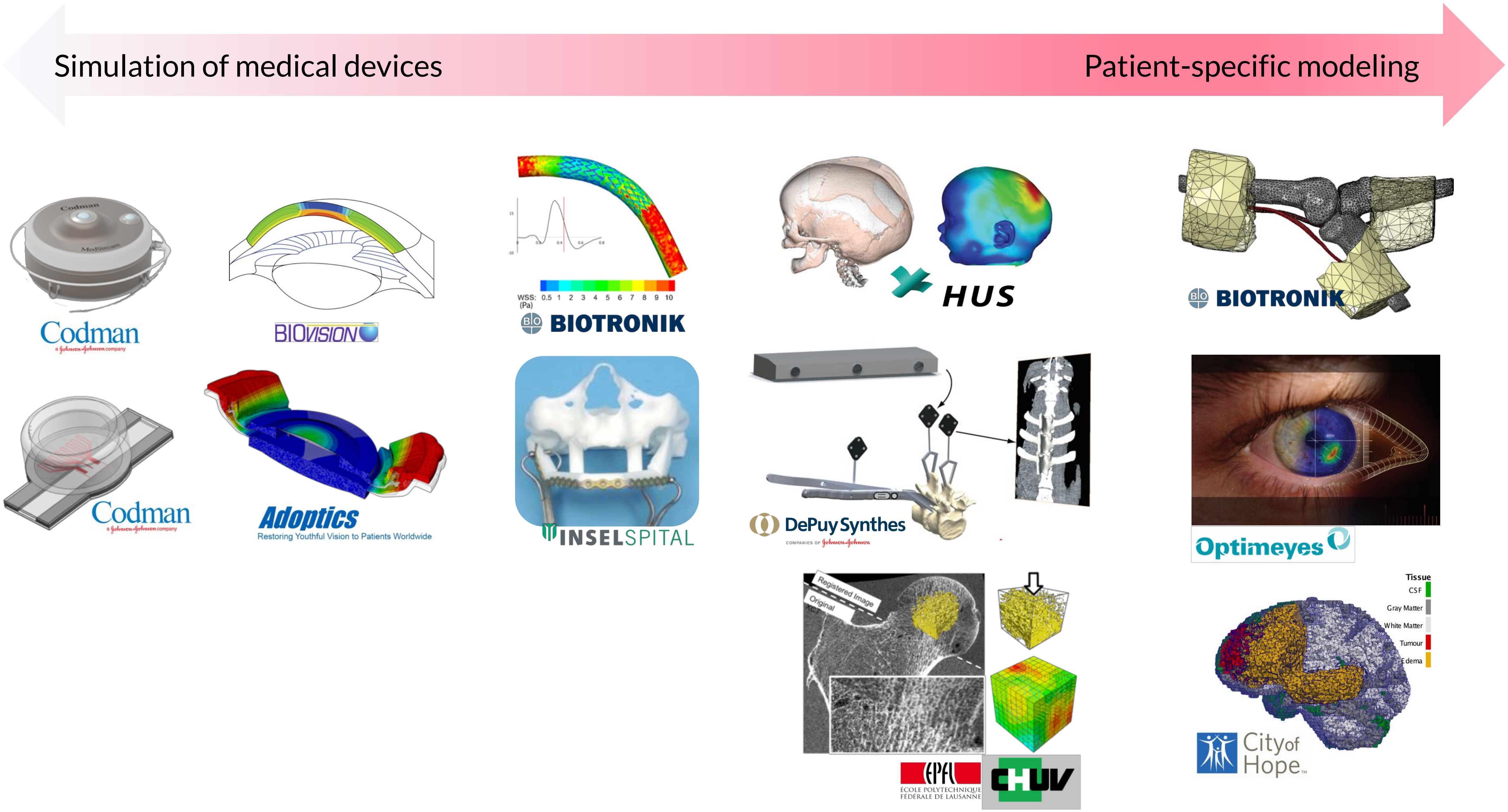
Simulation of medical devices
Patient-specific modeling
Codman
BIOVISION
WSS: 0.5 1 2 3 4 5 6 7 8 9 10
(Pa)
BIOTRONIK
HUS
BIOTRONIK
Codman
Adoptics
Restoring Youthful Vision to Patients Worldwide
INSELSPITAL
DePuy Synthes
Optimeyes
Registered Image
Original
EPFL
ÉCOLE POLYTECHNIQUE FÉDÉRALE DE LAUSANNE
CHUV
Tissue
CSF
Gray Matter
White Matter
Tumour
Edema
City of Hope

Simulation of medical devices

Patient-specific modeling

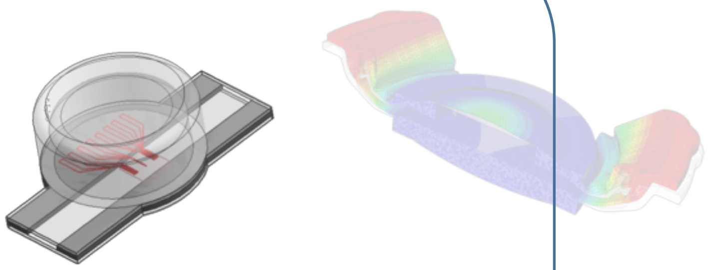

1. NEUROSURGERY

Thermal flowsensor for hydrocephalus

2. SPINAL SURGERY

Adolescent Idiopathic Scoliosis

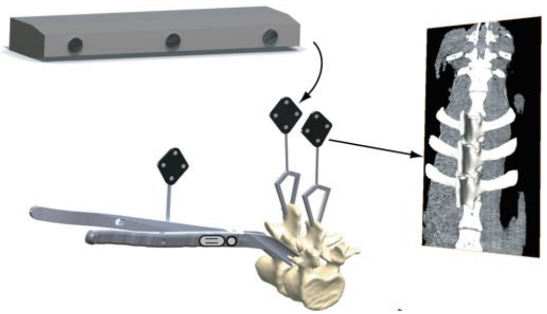

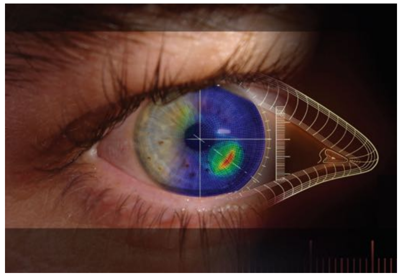

3. OPHTHALMOLOGY

Optimization of refractive interventions

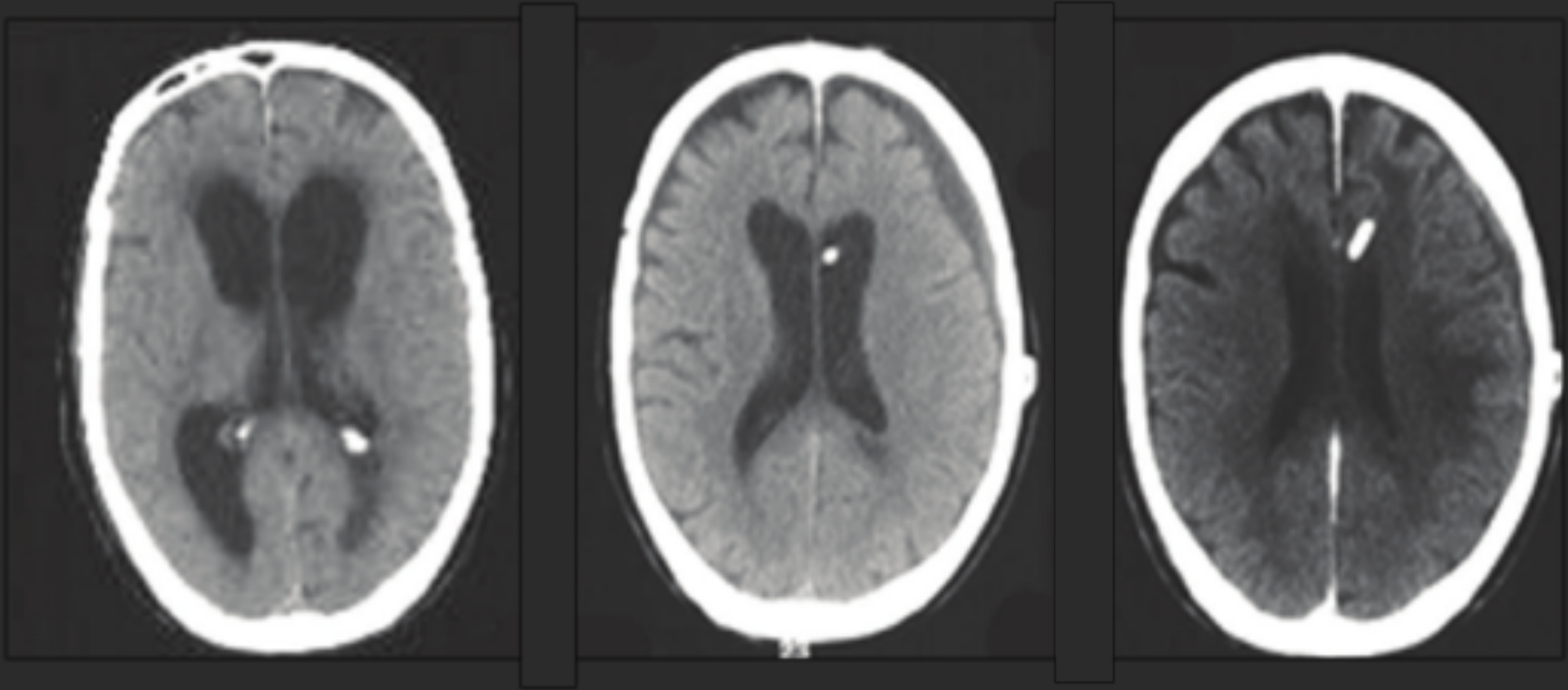

Finite Element Analysis of a CSF Flowsensor

Haute Ecole Arc, Neuchâtel – Bern – Jura
Bern University of Applied Sciences, Biel, Switzerland
Codman Neurosciences (J & J), Le Locle, Switzerland

Hydrocephalus

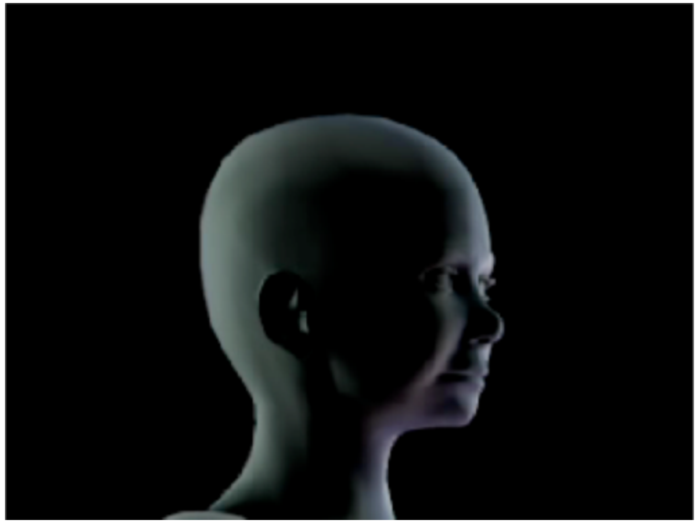

> Hydrocephalus
  - " Water in the brain "
  - Accumulation of Cerebrospinal fluid (CSF) in the brain
  - Production superior to absorption
  - Congenital malformation/ head injuries, infections
  - Occurs in 1 out of 500 live births

> Effects
  - Bulging of skull in young infants
  - Elevated intracranial pressure
  - Headaches, vomiting, nausea
  - Mental disability

Clinical treatment of hydrocephalus

- Shunt/catheter
  - drainage of the fluid
  - ventricular cavities to other body cavities

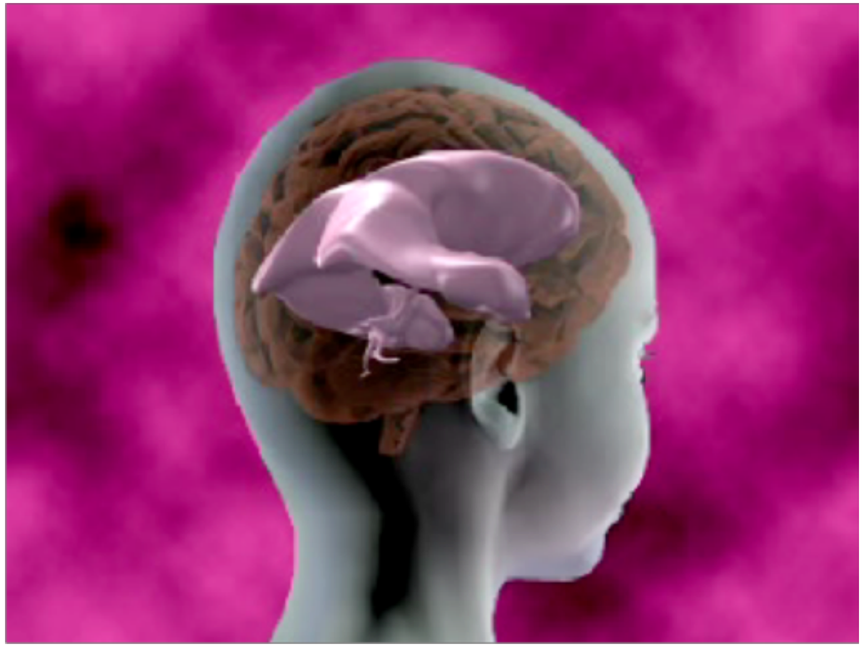

- Complications
  - 40% no complications
  - 30% overdrainage
  - 20% shunt blocked
  - 10% infections

Thus the need for a flow sensor

Thermal flowsensor

Measure of the flow based on temperature difference between two sensors

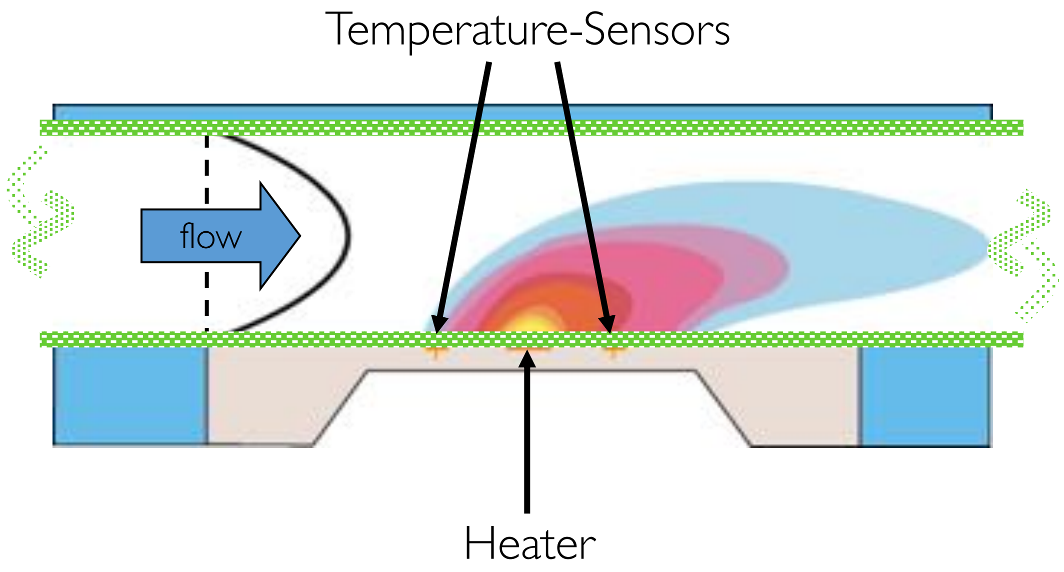

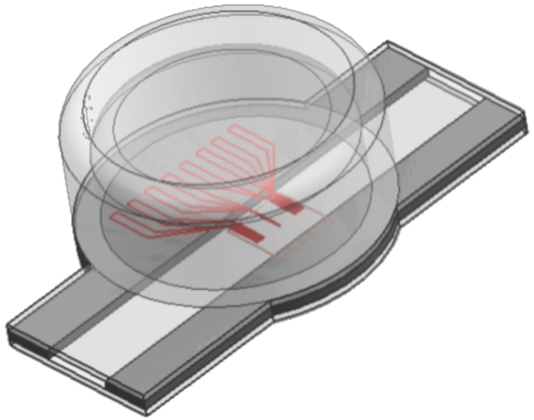

Finite element analysis

- Criteria : Sensor could have
  3 different accuracy schemes
  - 0 - 2ml/h: detect zero flow
  - 2 - 40ml/h: maximum of accuracy
  - 40 - ~300ml/h: detection but less accurate
- 40’000 elements
- Combines heat transfer with flow

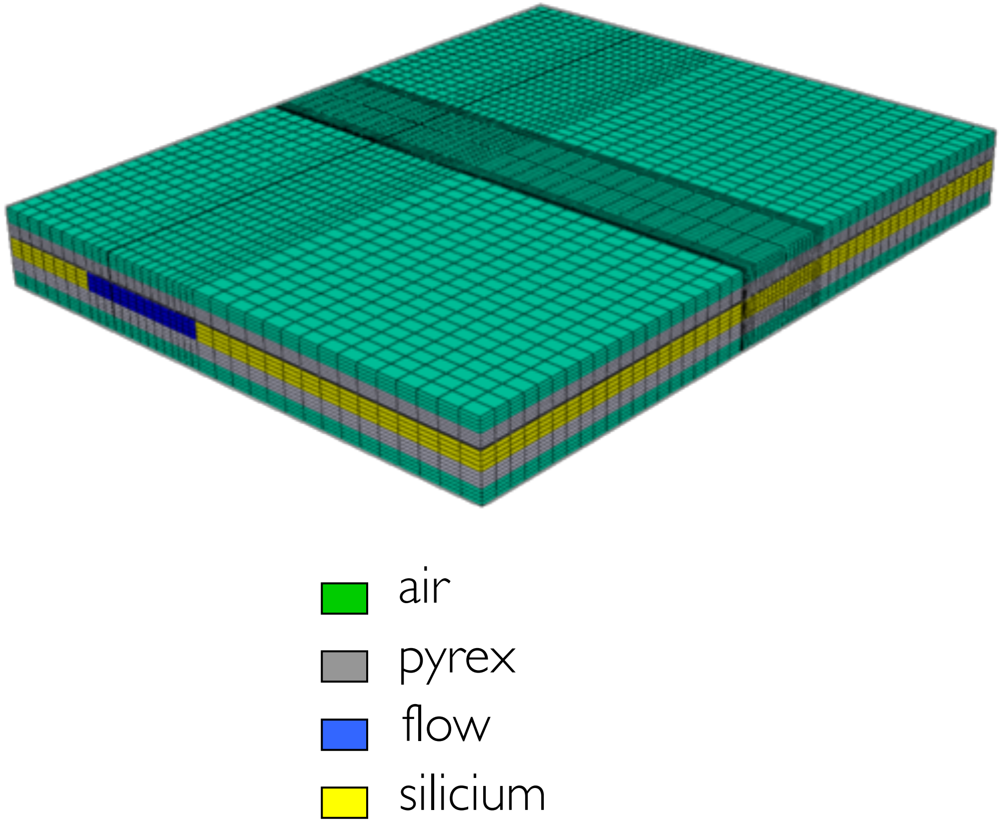

Validation

- Measurements taken on 5 different sensors with 2 different heating power
- Values taken every 1ml/h

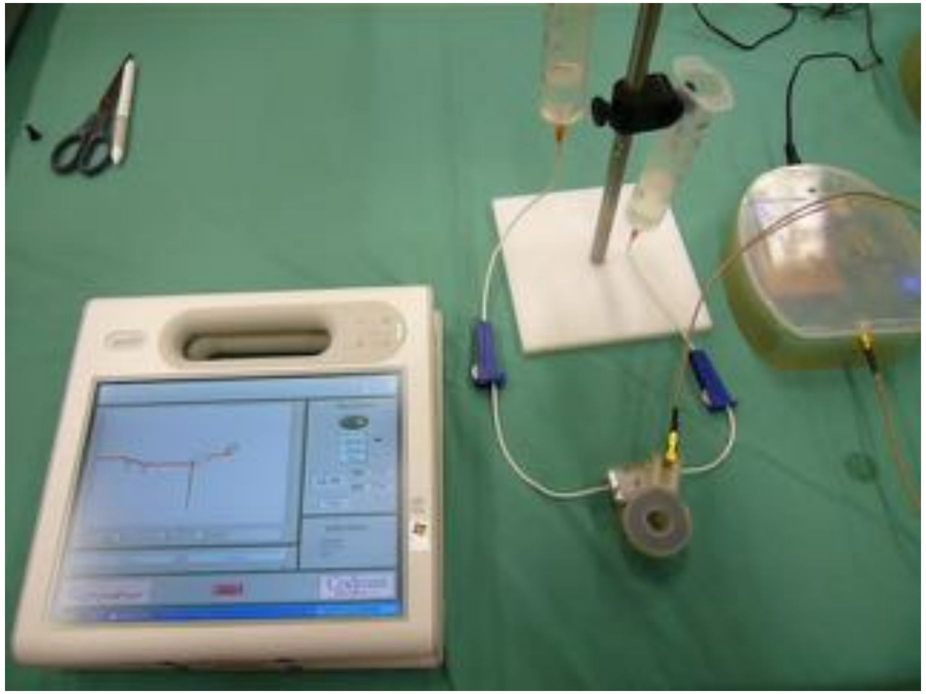

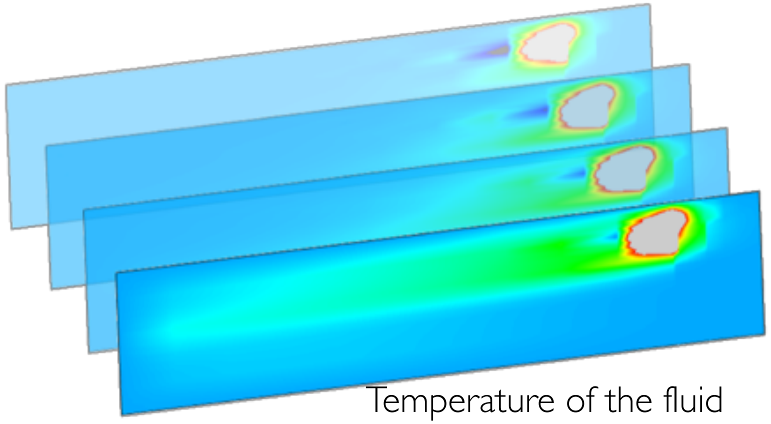

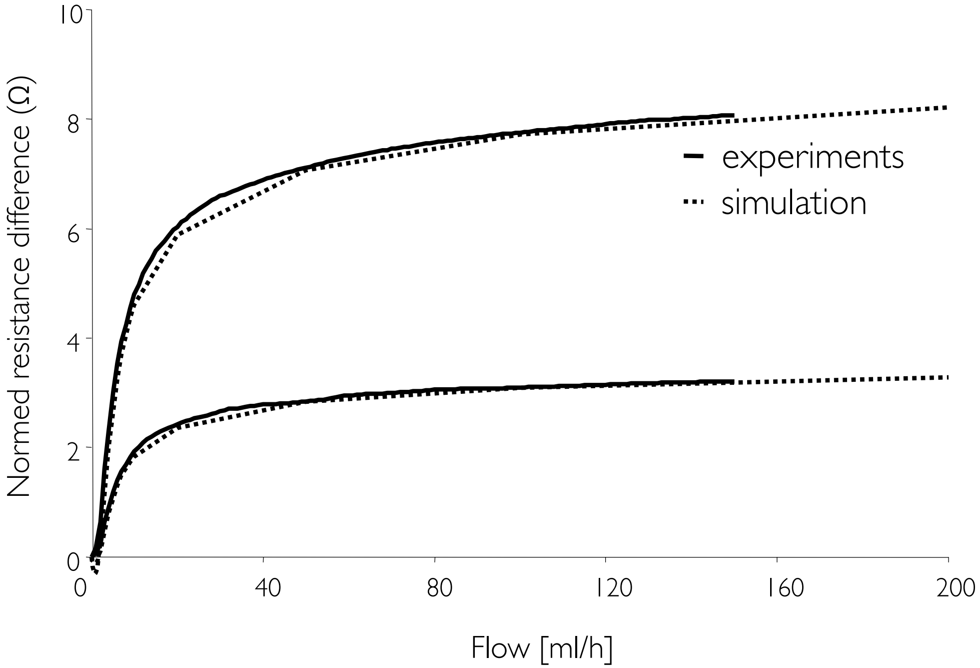

Symmetric vs. antisymmetric configurations

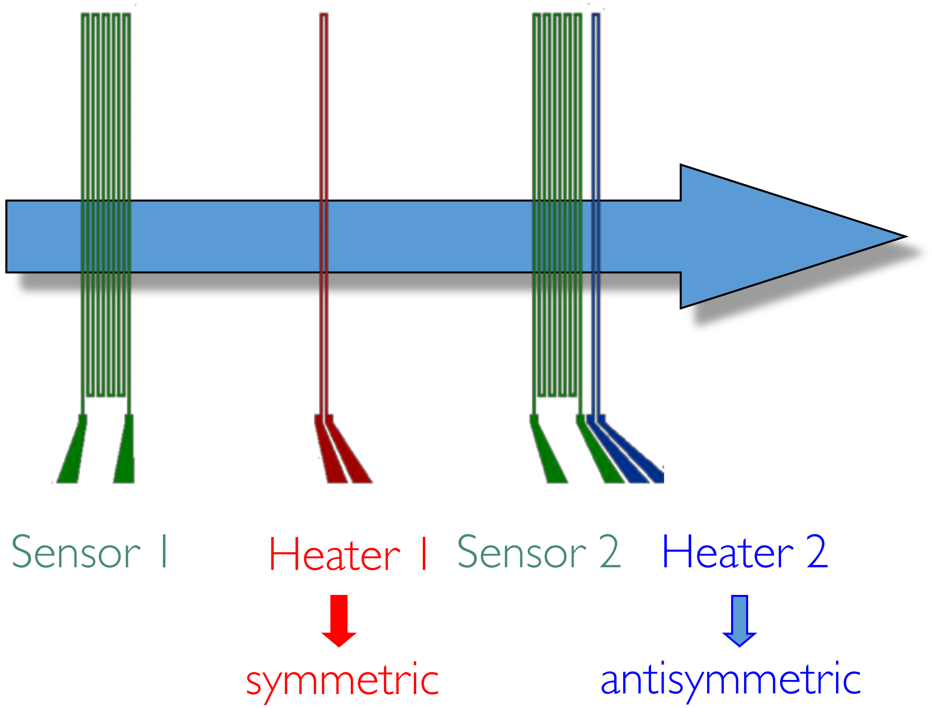

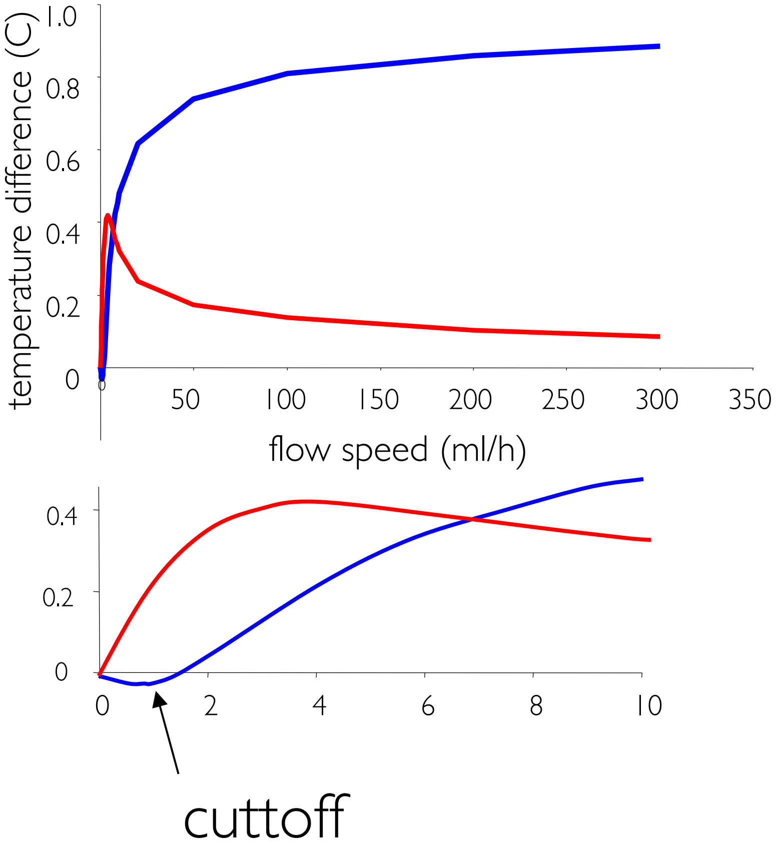

> Antisymmetric design is more appropriate
> Maximize temperature difference
> Minimize cuttoff

Influence of sensors positionning

- Tests with some typical cases
  - existing configuration (1)
  - furthest sensor – closest sensor (2)
  - closest sensor – closest sensor (3)

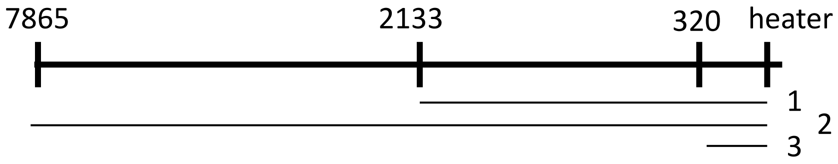

	1	2	3
Cuttoff (ml/h)	1.5	0	15
Temp diff range (C)	0.98	1.217	0.195

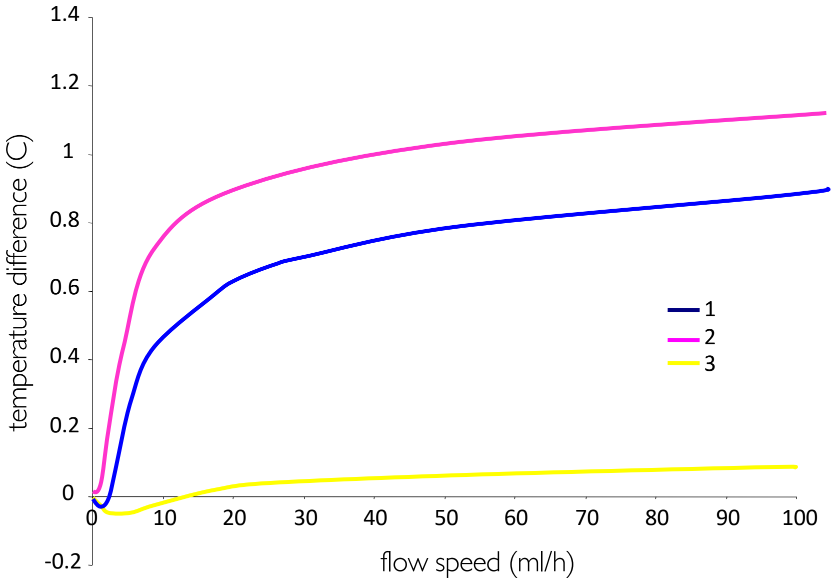

- Moving away the left sensor improves the behavior of the device

Influence of “trenches”

- Three cases studied:
  - Trench around the heater
  - Trench around the heater and the sensor
  - Trench around the sensor next to the heater

Trench mode	Max Temp. Difference	Cutoff
Heater	2.17	1.15
Heater and sensor	2.66	1.75
Sensor	2.23	0.8

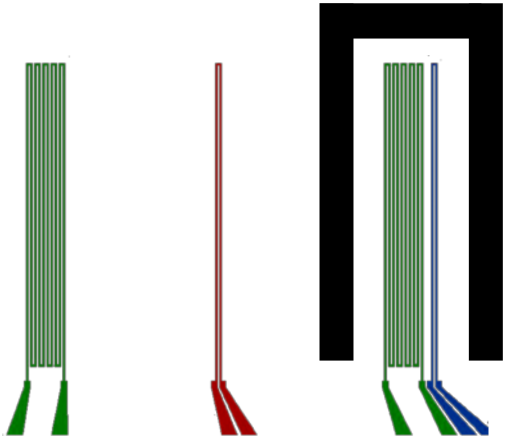

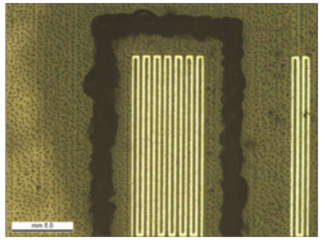

- Best temperature difference with trench around heater and sensor
- Best cutoff when the trench around the sensor

Conclusions

> FEM effective tool for parametric evaluation / design optimization

> Optimal configuration determined

- Antisymmetric design
- Moving the left sensor away from heater
- Trenches around heater and sensor

Adolescent Idiopathic Scoliosis

DePuy Synthes

PART OF THE Johnson & Johnson FAMILY OF COMPANIES

UKBB

kompetent & menschlich

www.teenvogue.com

Adolescent Idiopathic Scoliosis

- Bone fusion (degenerative diseases and spinal deformities)
- Based on static, load-sharing principles
- Novel treatments based on motion-preserving implant
- Requires knowledge about the kinematic and dynamic behavior
- Experiments performed on spinal loading simulators
    + Application of pure moments
    + Controlled experimental conditions
    - Testing an isolated spine
    - Cadaver specimens with a certain pathology not available

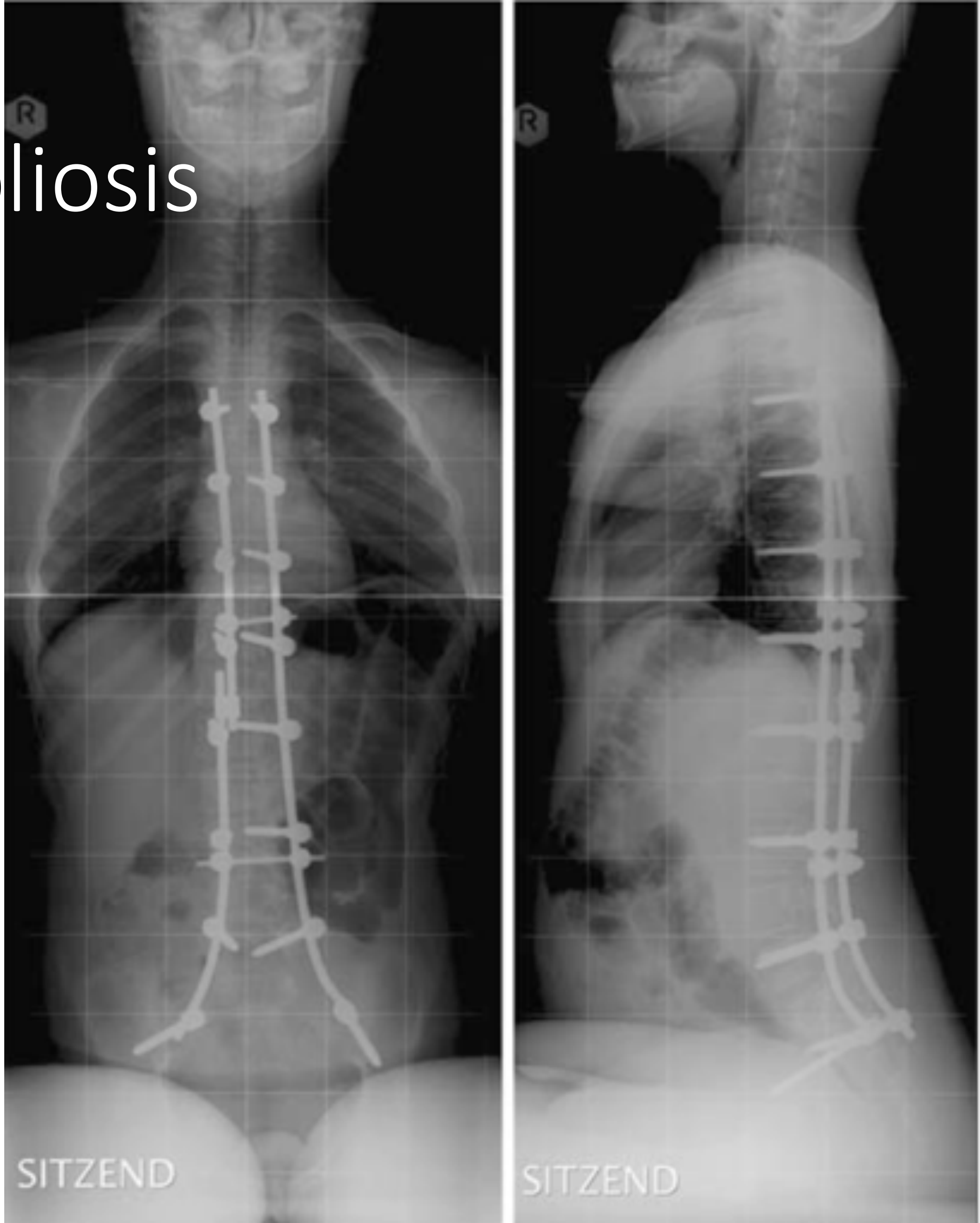

General measurement concept

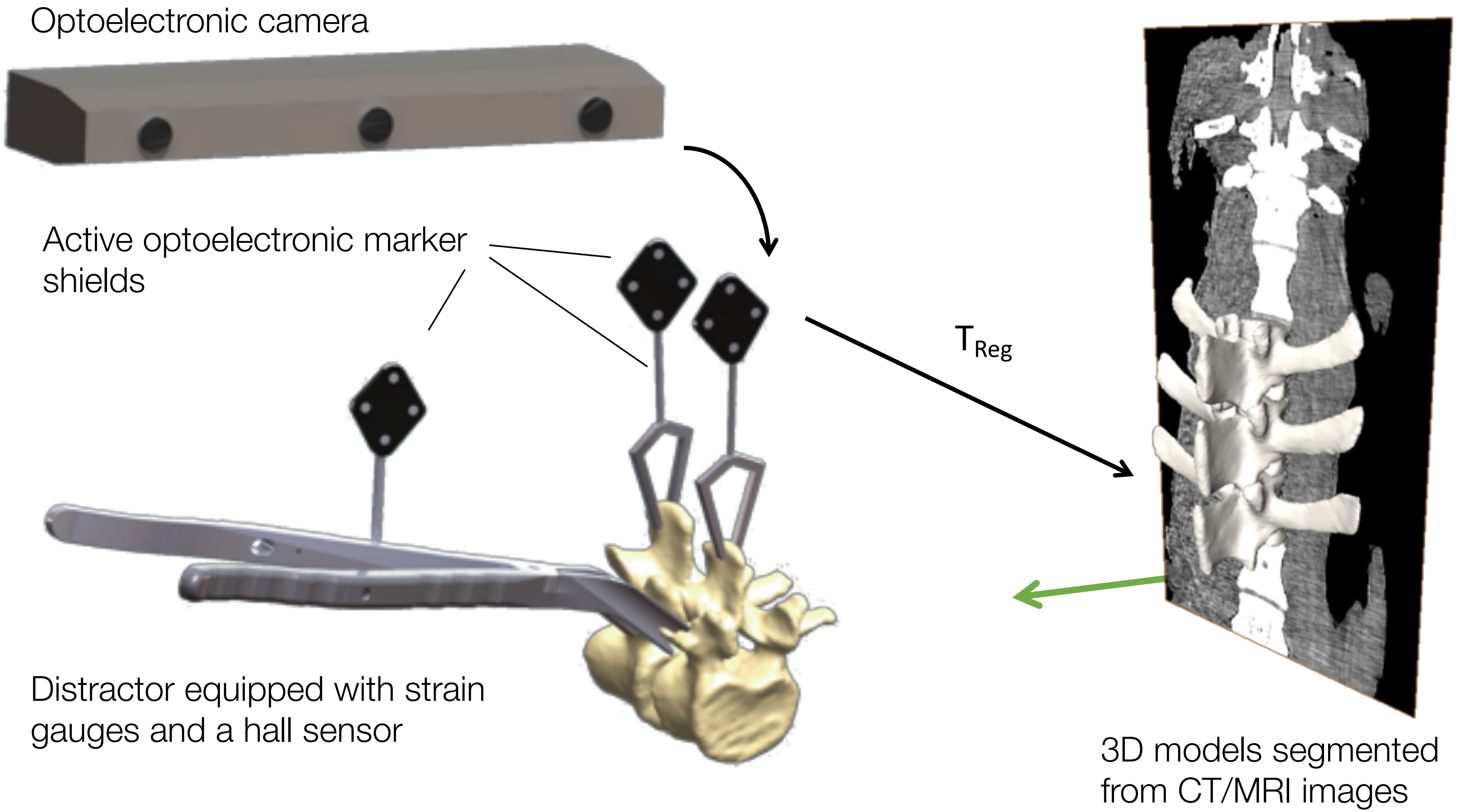

Intraoperative measurements

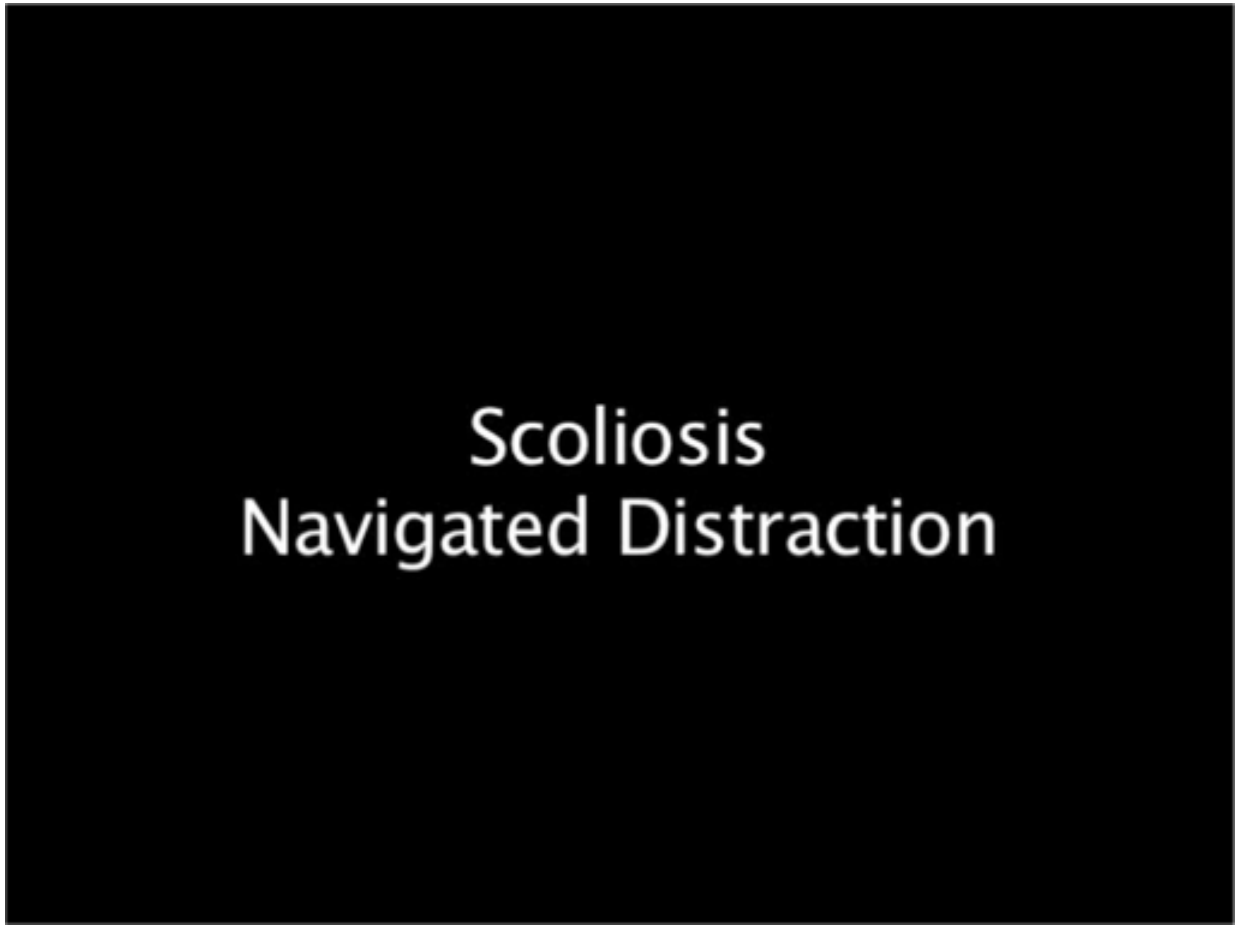

Results of one load cycle

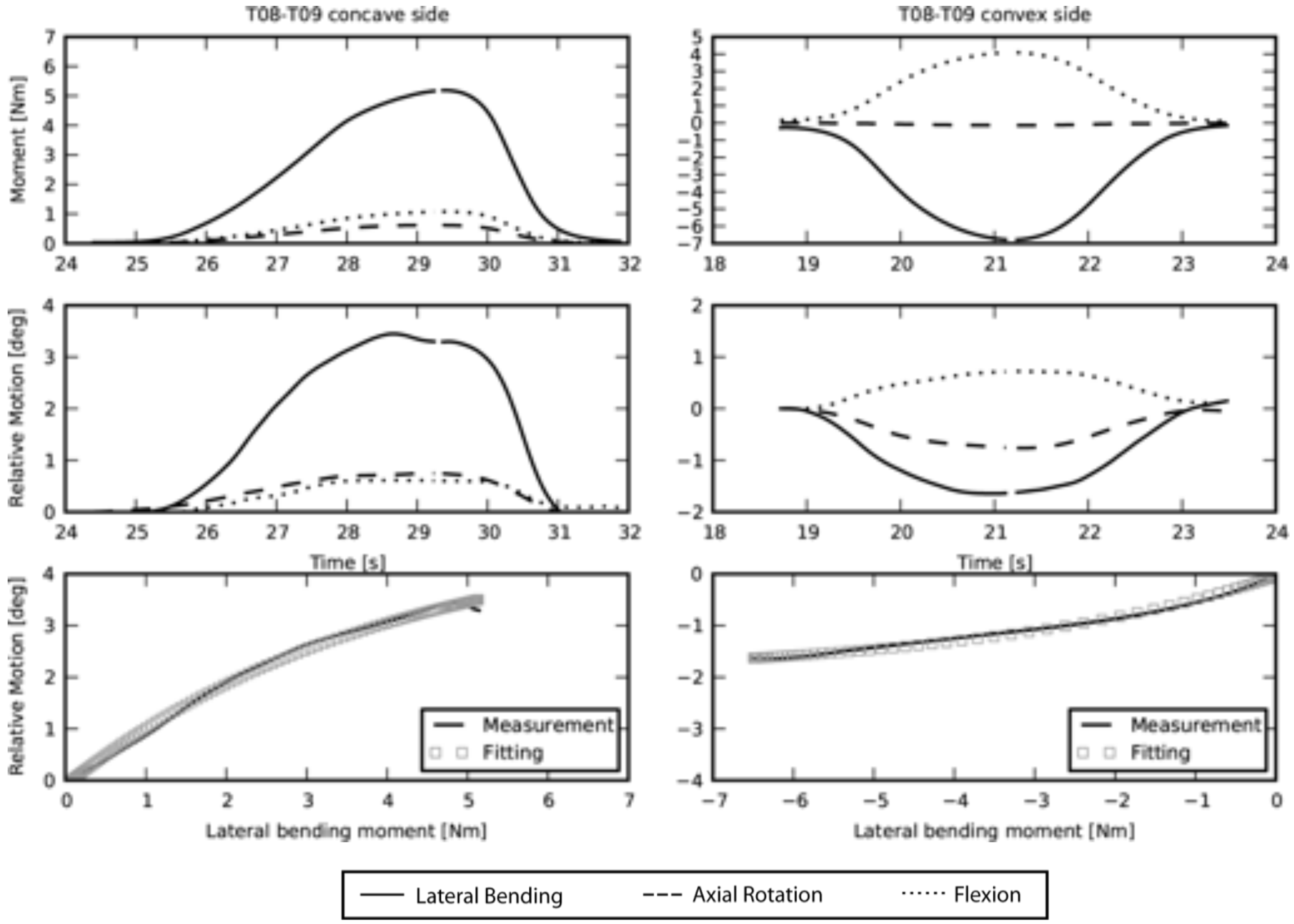

Results of one patient

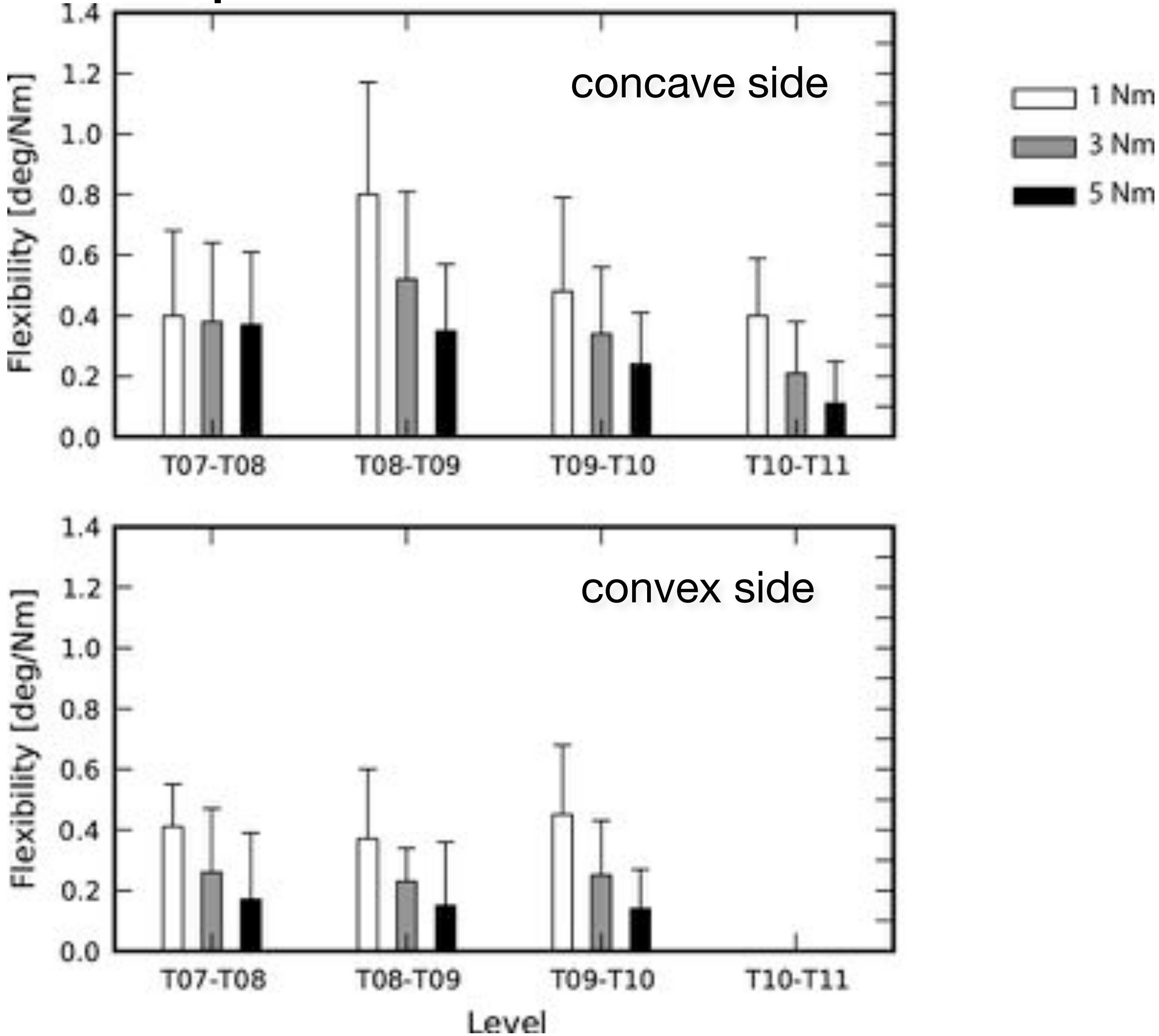

Numerical model – Posterior segment

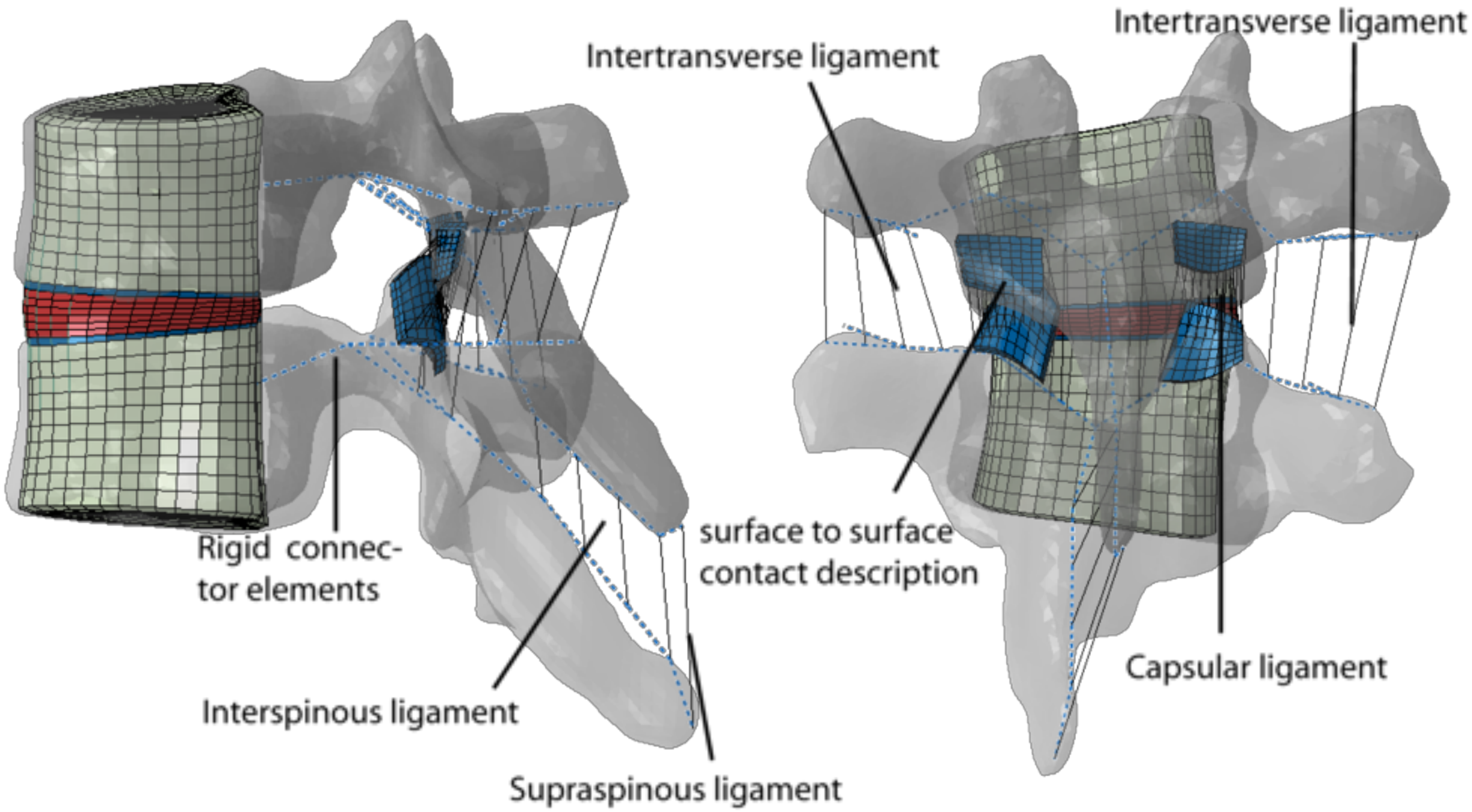

Optimization of mechanical parameters

> Strain energy density function

$$\psi = \underbrace{\frac{1}{D}(J-1)^2 + C_{10}\left(\bar{I}_1 - 3\right)}_{\text{Ground matrix}} + \underbrace{\frac{\mu}{\gamma}\left(I_4^{\gamma/2} - 1\right) - \mu \ln I_4^{\gamma/2}}_{\text{Fiber contribution}}$$

> Parameter vector

$$\kappa = \begin{pmatrix} C_{10} & \gamma_{Lig} & \gamma_{LigConvex} & \gamma_{AnnuConvex} & \gamma_{AnnuConcave} \end{pmatrix}$$

> The cost function includes the 3 Euler angles for “convex” and “concave” experimental data:

$$f(\kappa) = \sum_{i=1}^{3} \| W_i(u_i(\kappa) - u_i{}^{exp} \|^2 \rightarrow \min$$

UNIVERSITÄT BERN

Finite element simulations

- Force applied on the transverse process of the concave side

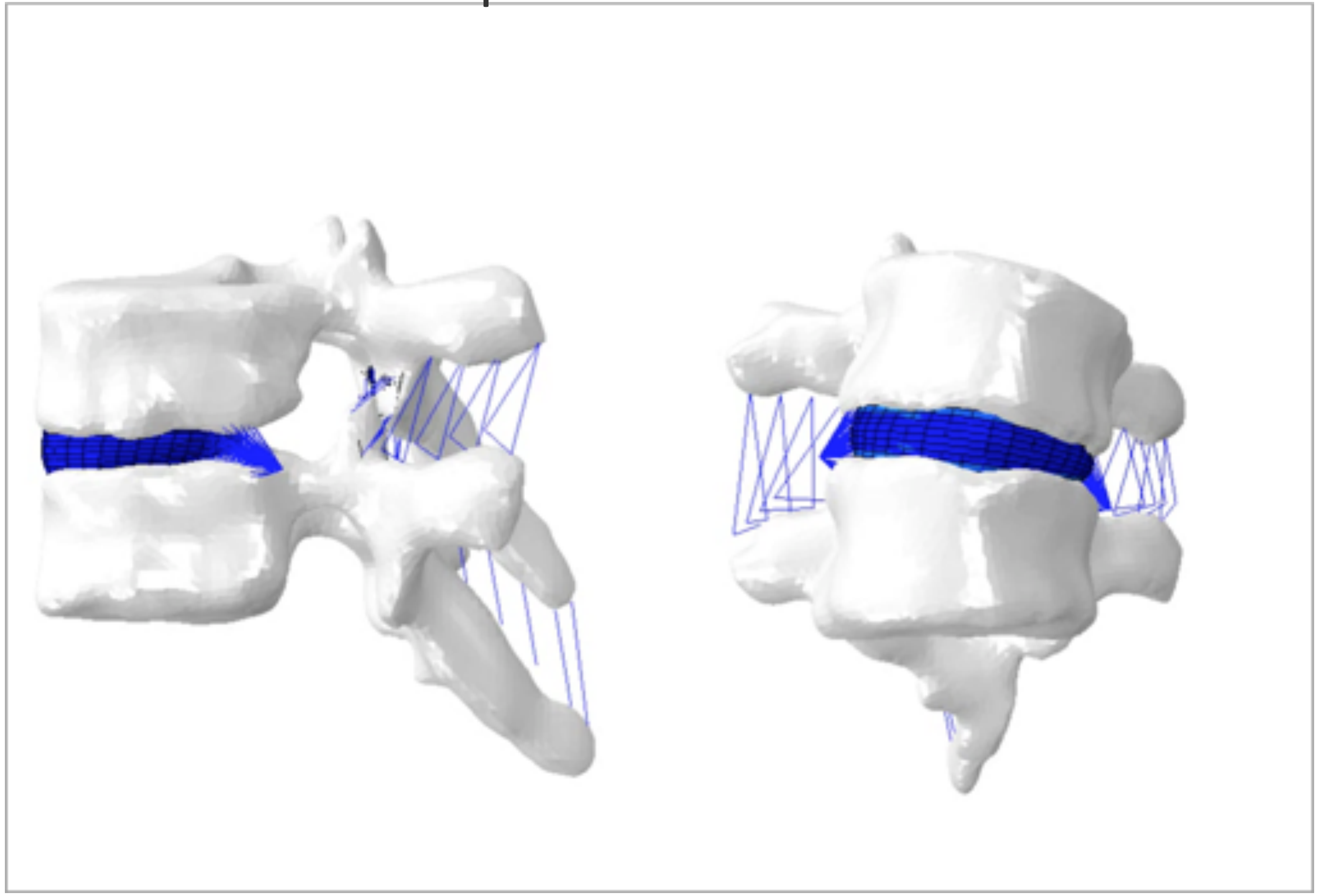

Optimized parameters (one segment)

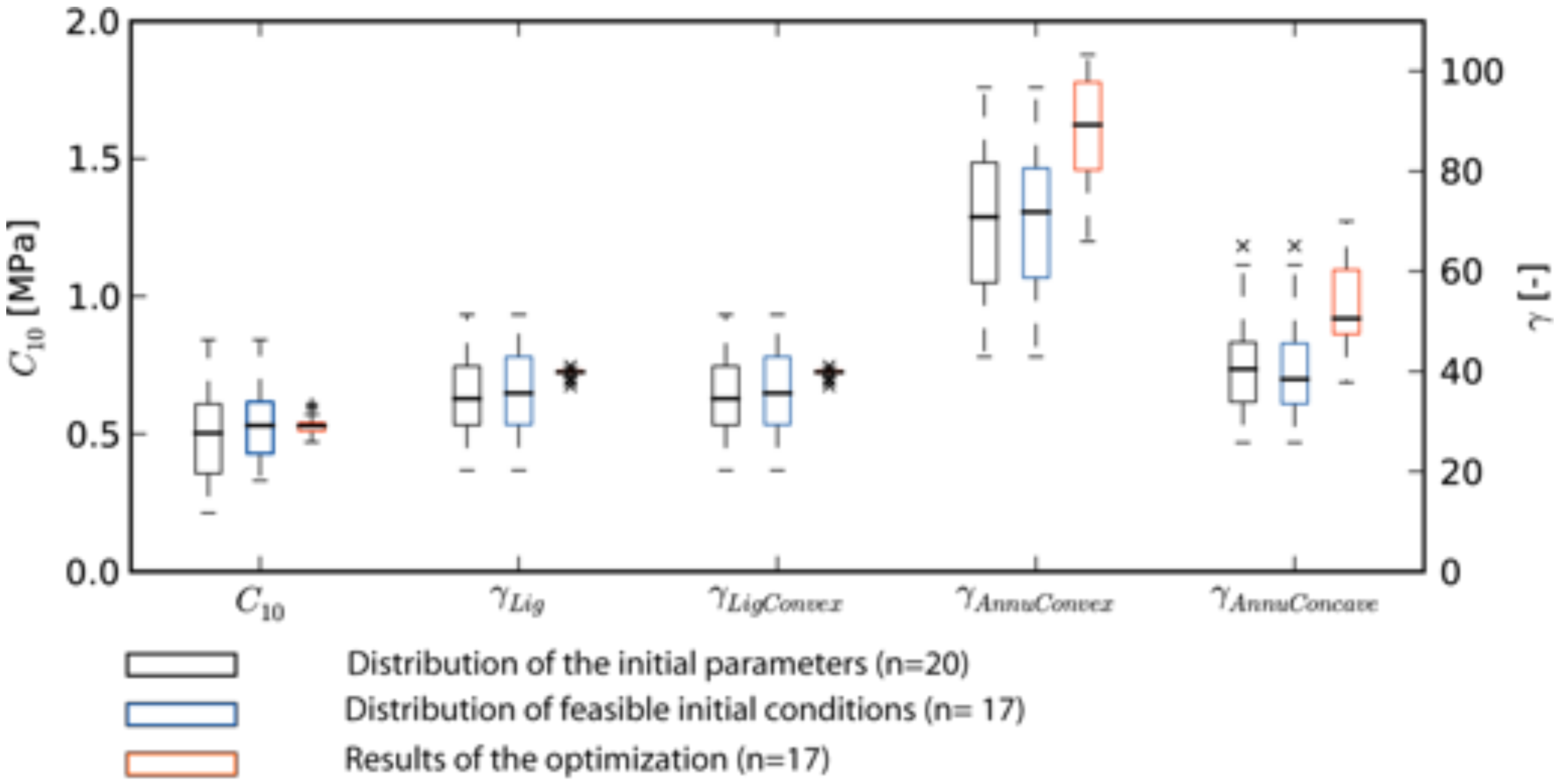

Simplified model of the intervertebral disc

> A nonlinear stiffness matrix used to simplify the disc model

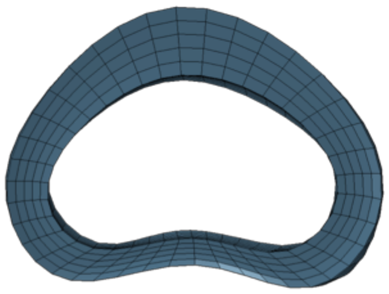

$$\begin{pmatrix} K_{11} & K_{12} & K_{13} \\ K_{21} & K_{22} & K_{32} \\ K_{31} & K_{23} & K_{33} \end{pmatrix} \begin{pmatrix} \alpha \\ \beta \\ \gamma \end{pmatrix} = \begin{pmatrix} M_1 \\ M_2 \\ M_3 \end{pmatrix}$$

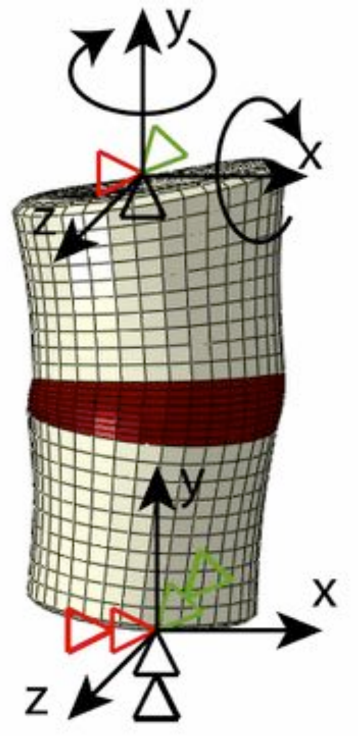

> Basic load cases to "populate" the stiffness matrix

> Implemented as a User Element in Abaqus

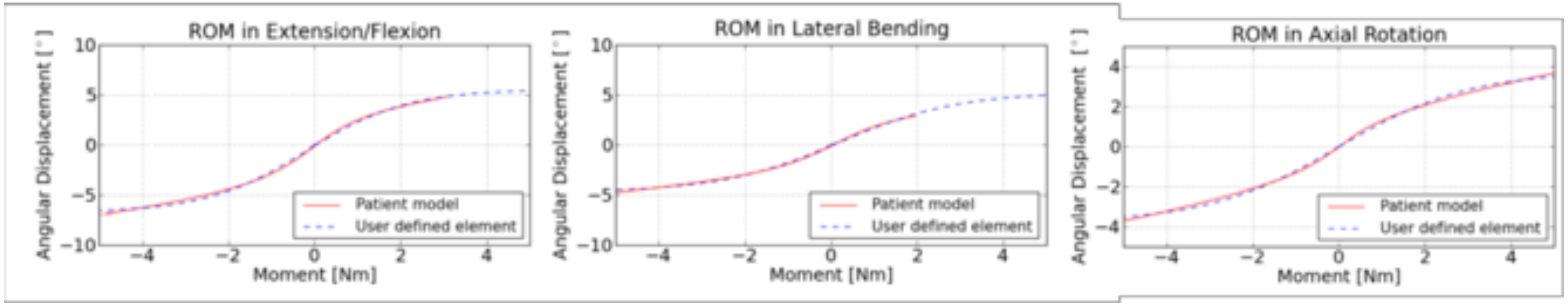

Multi-Segment (Global) Model

> 12 Vertebrae
> Facet joints
> All major ligaments
> Intervertebral disc
> Rigid connection between the ribs and sternum.
> Costotransverse and the costovertebral joints modeled
> T4 moves vertically
> L3 Fixed

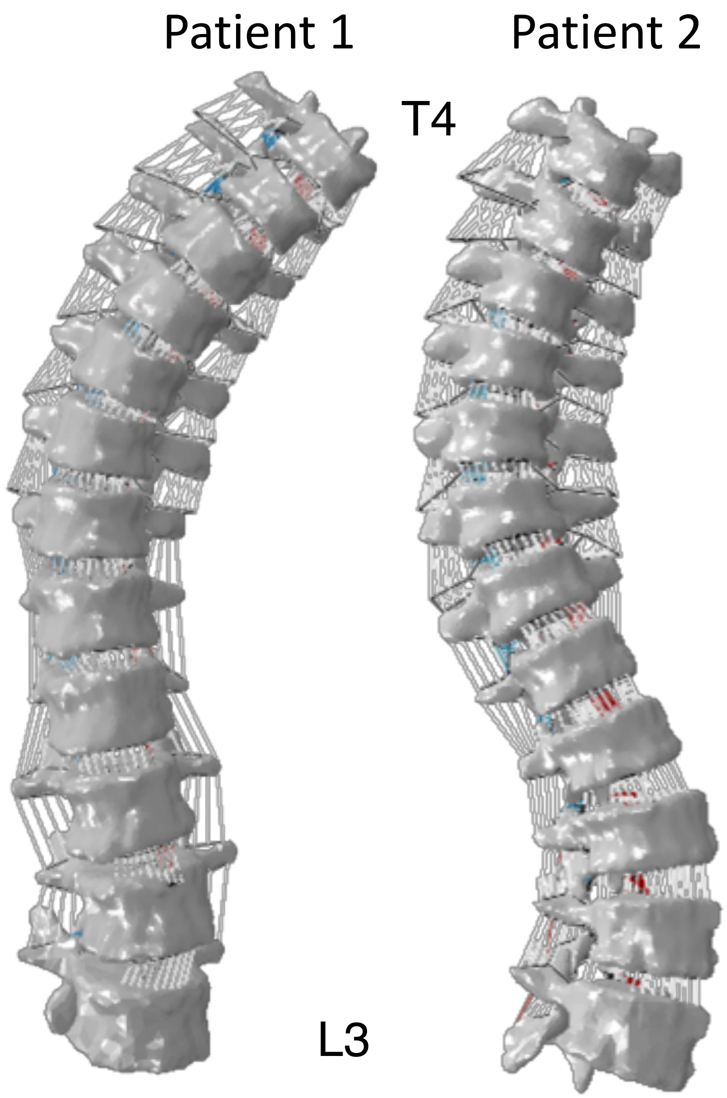

Validation

UNIVERSITÄT BERN

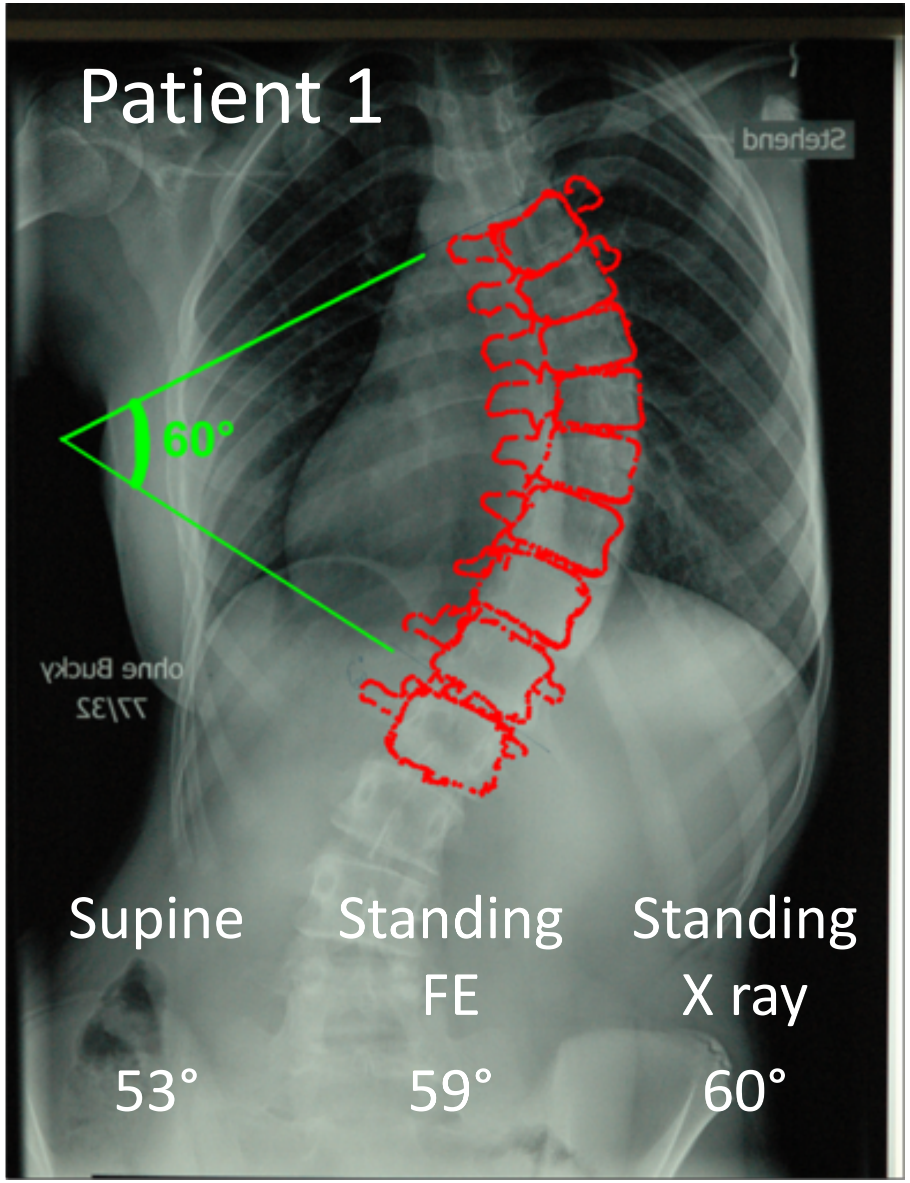

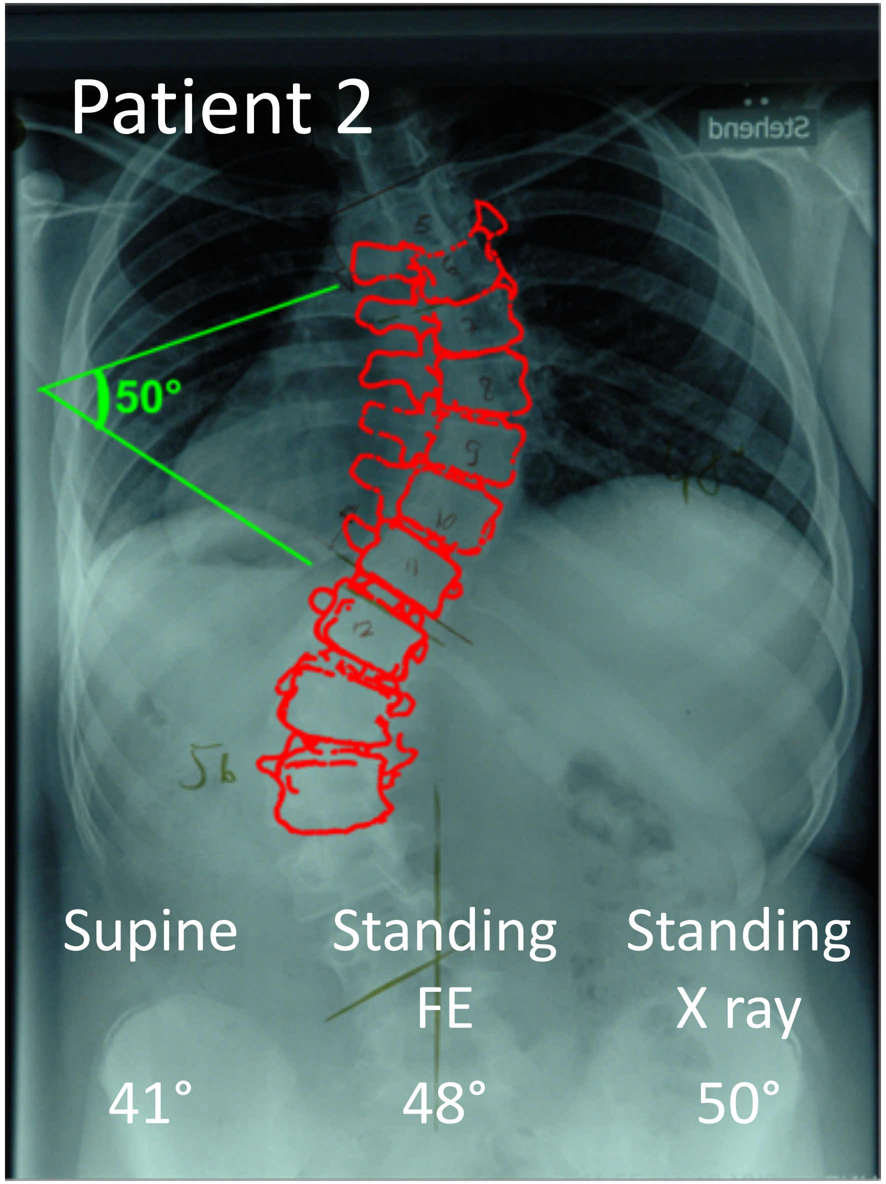

Position and Degrees of Freedom (DoF)

- **Implant Length**: Long or Short
- **Upper Point**: Variable Position & Variable DoF
- **Lower Point**: Variable DoF but Position is Constant

Lateral Position

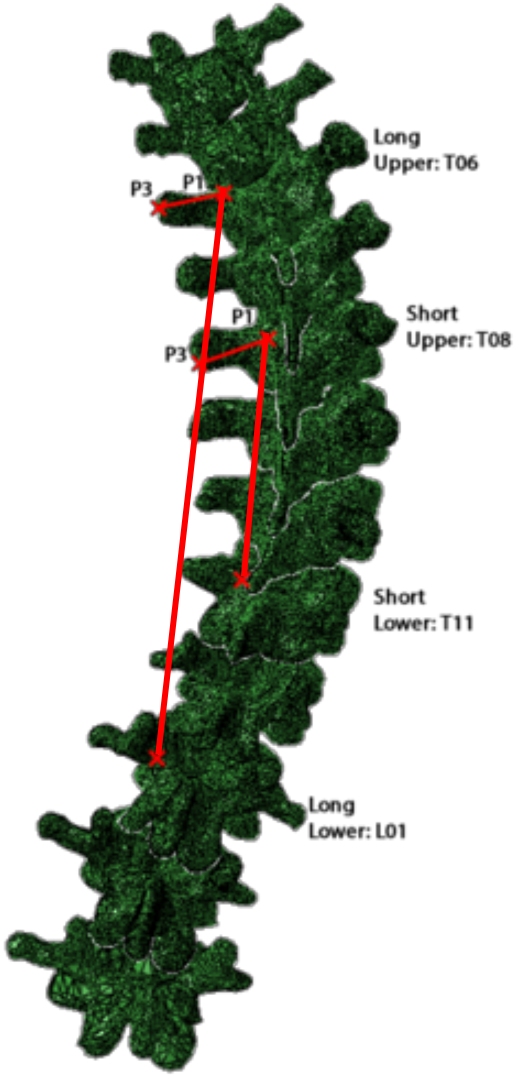

Posterior Position

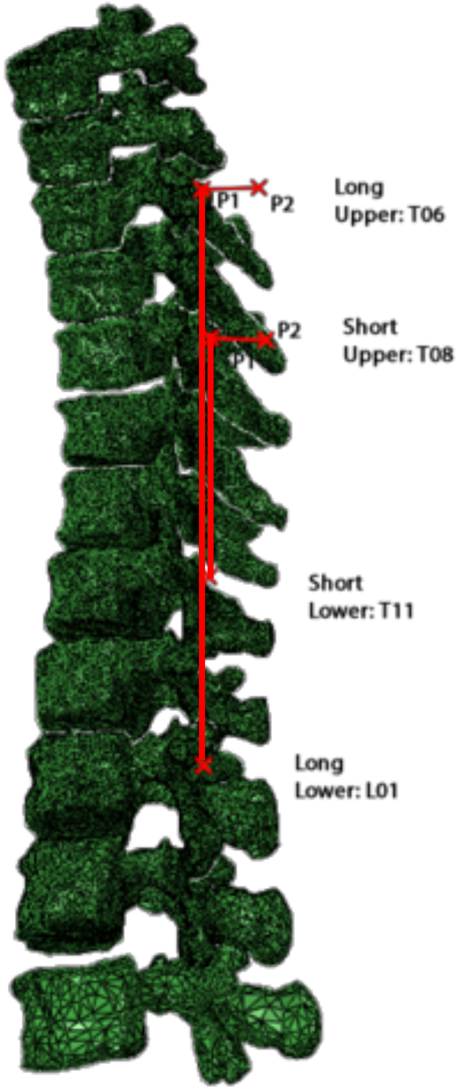

Planned correction (short growing implant)

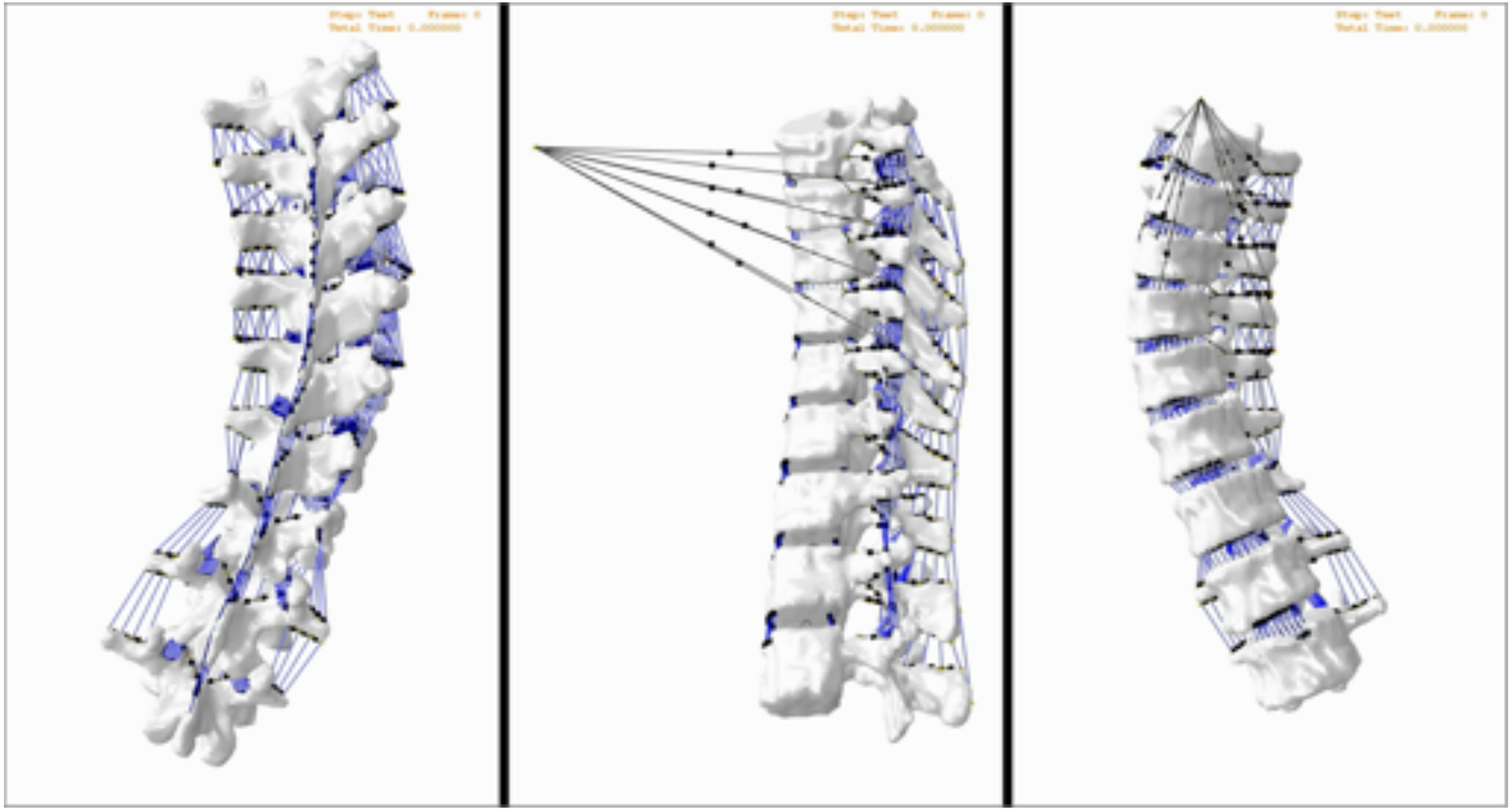

How can we assess the spinal stiffness

of a given subject

in a non-invasive way

and before the surgery

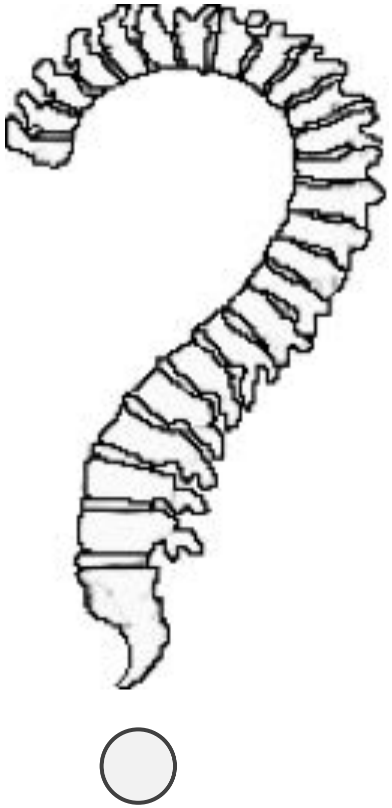

Method: overview

- Apply a load on the spine
- Measure its displacement & the load
- Derive patient's stiffness

$$\{\phi\} = [K]^{-1}\{F\}$$

- $\{\phi\}$ ↑ Imaging techniques
- $[K]$ ↑ ? Patient
- $\{F\}$ ↑ Body weight distribution

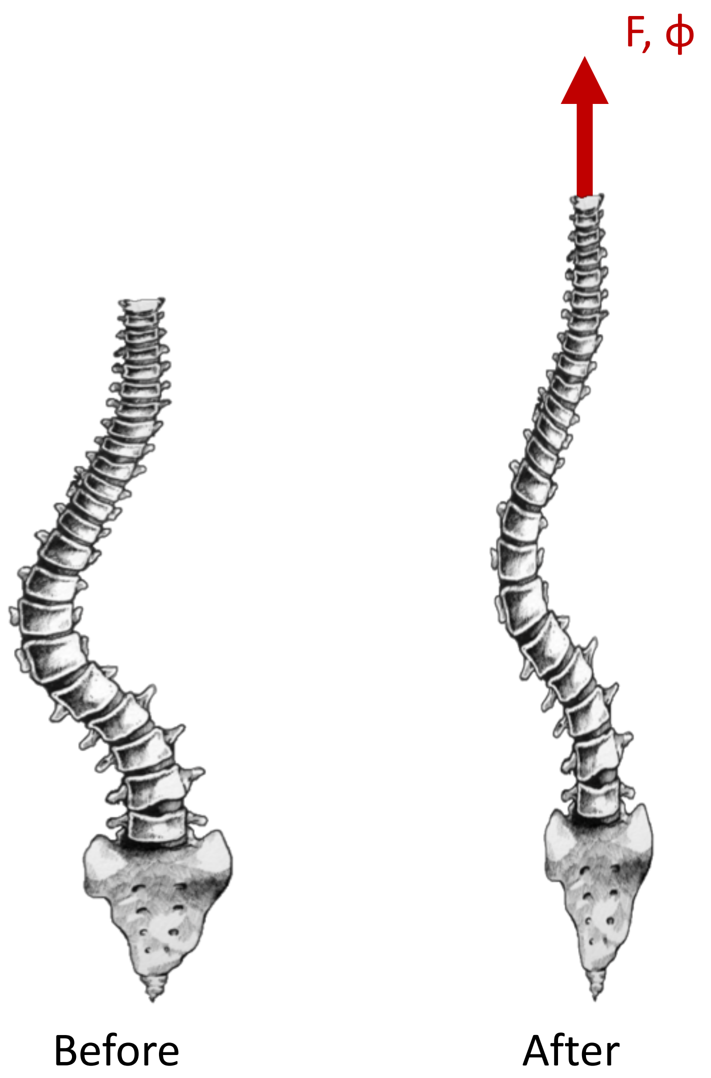

Spinal Traction

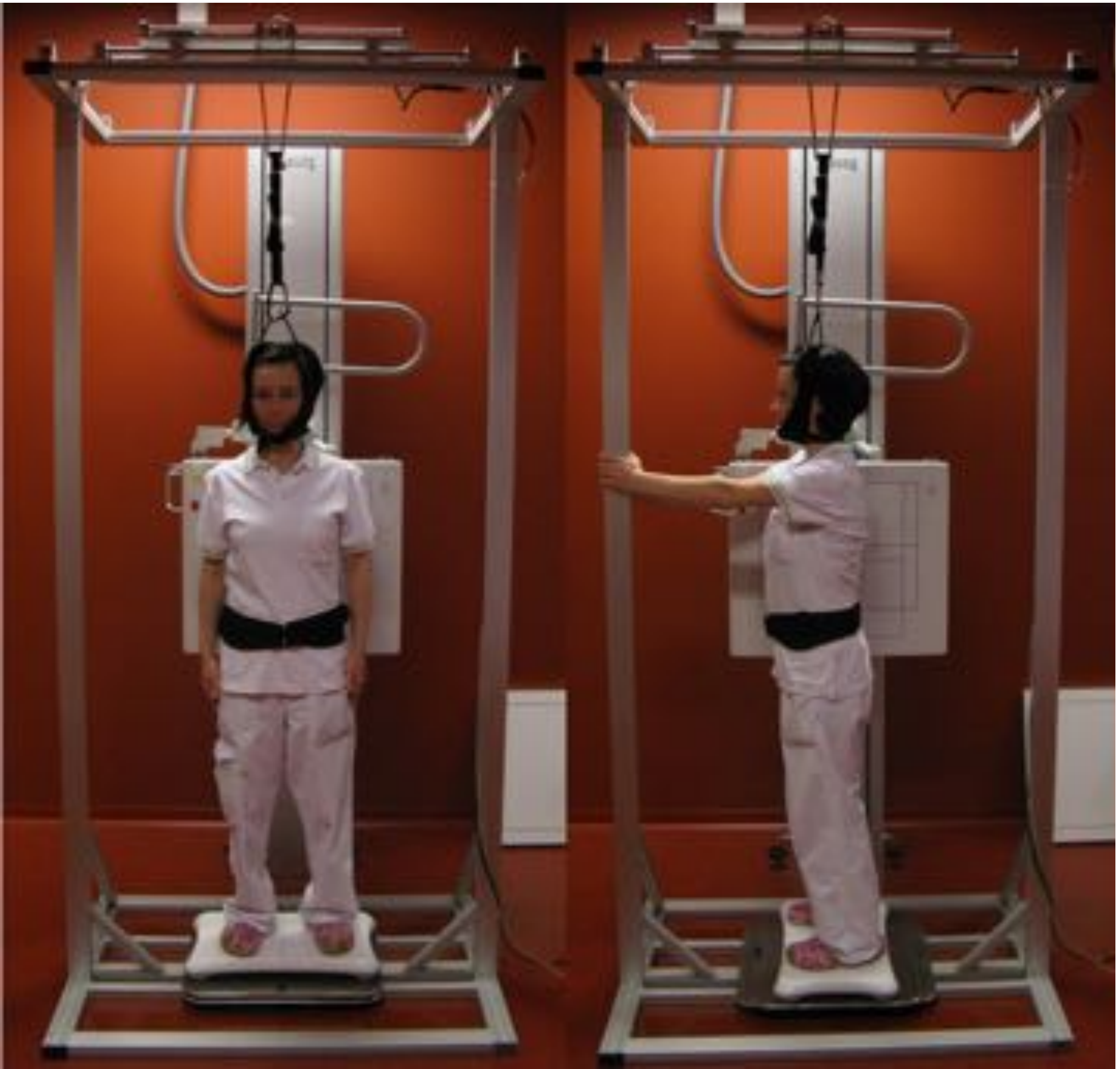

- The traction force is applied to the head, therefore **the load is directly transmitted to the spine**
- A frictionless platform guarantees the axial alignment of the load with the spine
- The **load equals 30%** of the patient's BW

5 Patients

UNIVERSITÄT BERN

Subjects	Age [years]	Weight [Kg]	Apex location	Apex rotation "standing"	Cobb Angle "standing"
1	15	59.3	L1	43°	67°
2	16	56.3	T9	38°	71°
3	13	53.6	T8	28°	46°
4	18	48.1	T8	31°	50°
5	15	57.0	L1	34°	60°

UNIVERSITÄT BERN

Results of the traction

Patient 1 | Patient 2 | Patient 3 | Patient 4 | Patient 5

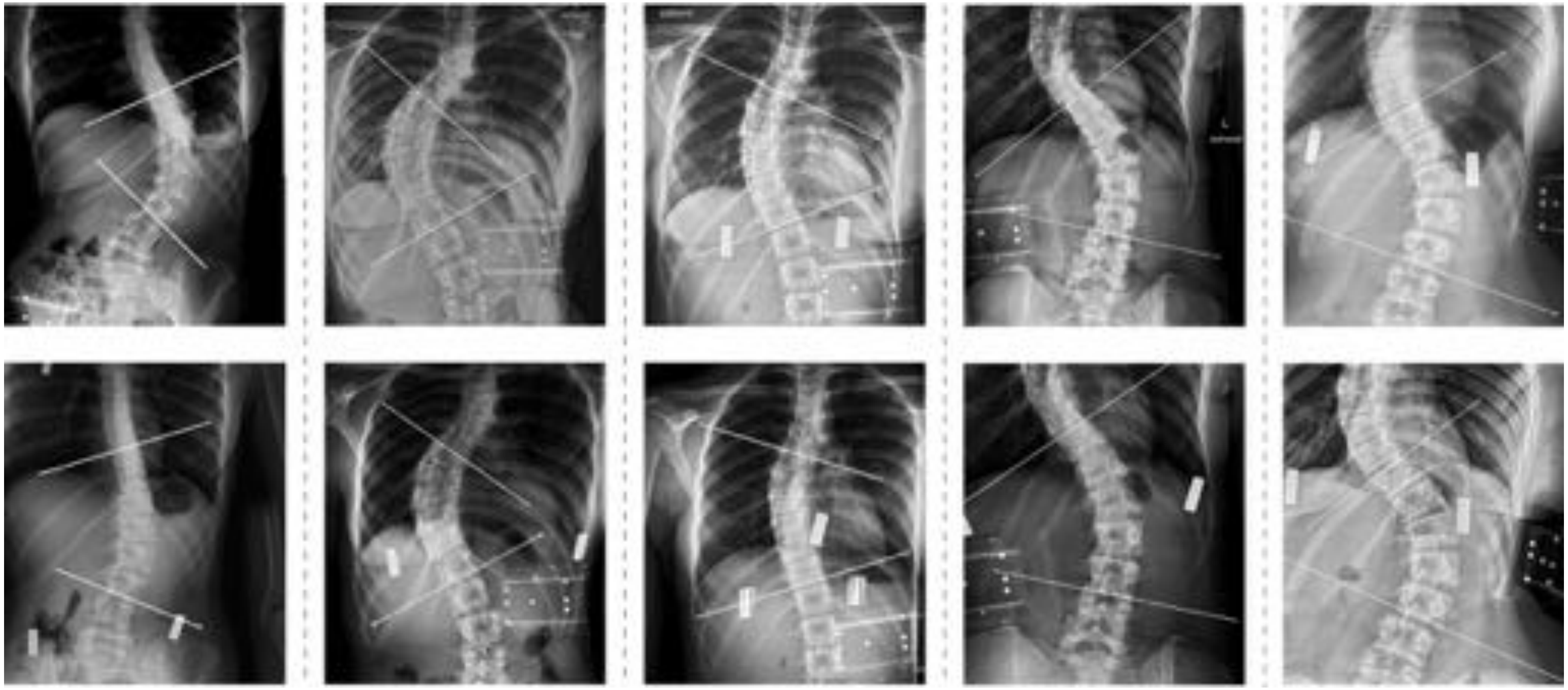

2D / 3D reconstruction

1) **Experiment**

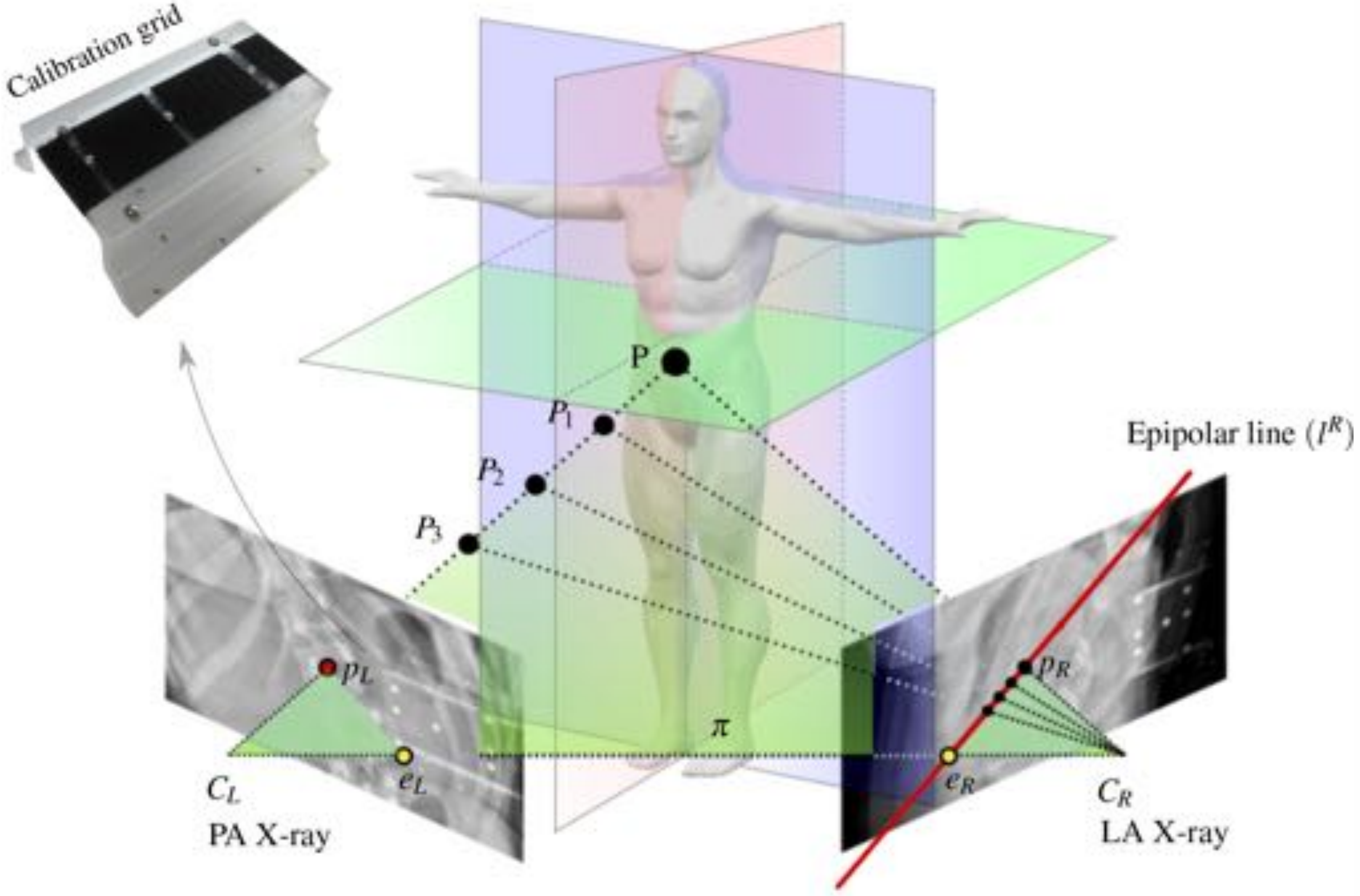

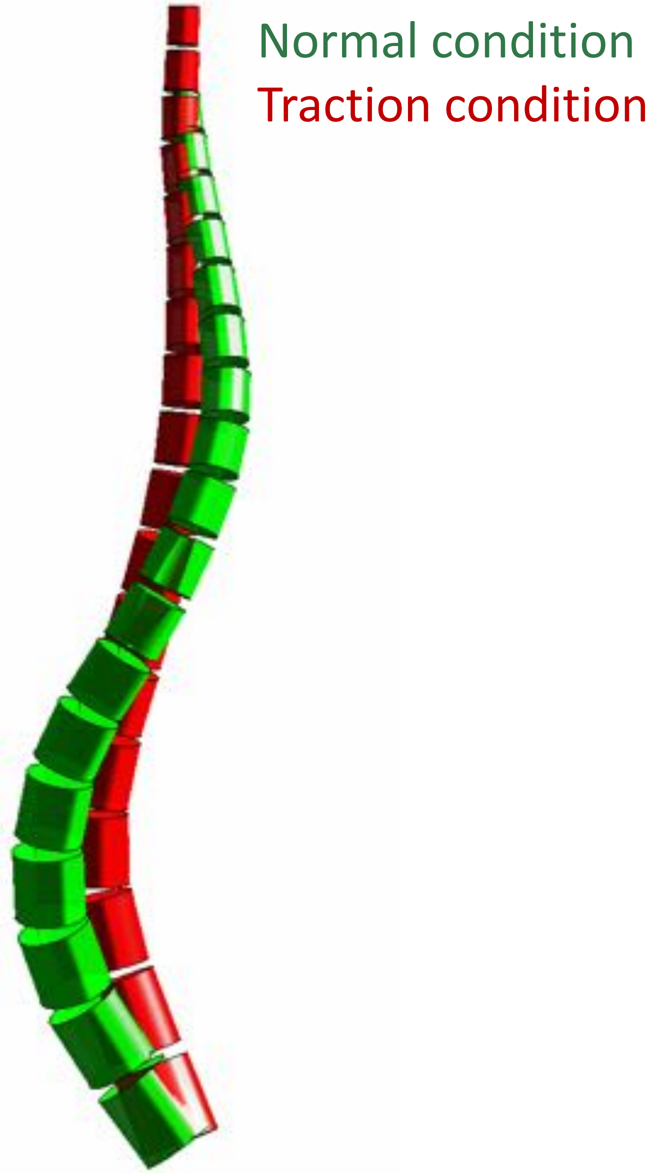

"Beam" FEM Model

1) Experiment

- Apply a load on the spine
- Measure its displacement & the load

2) Model

- Create a FEM of the spine in normal condition

3D reconstructed spine in normal condition

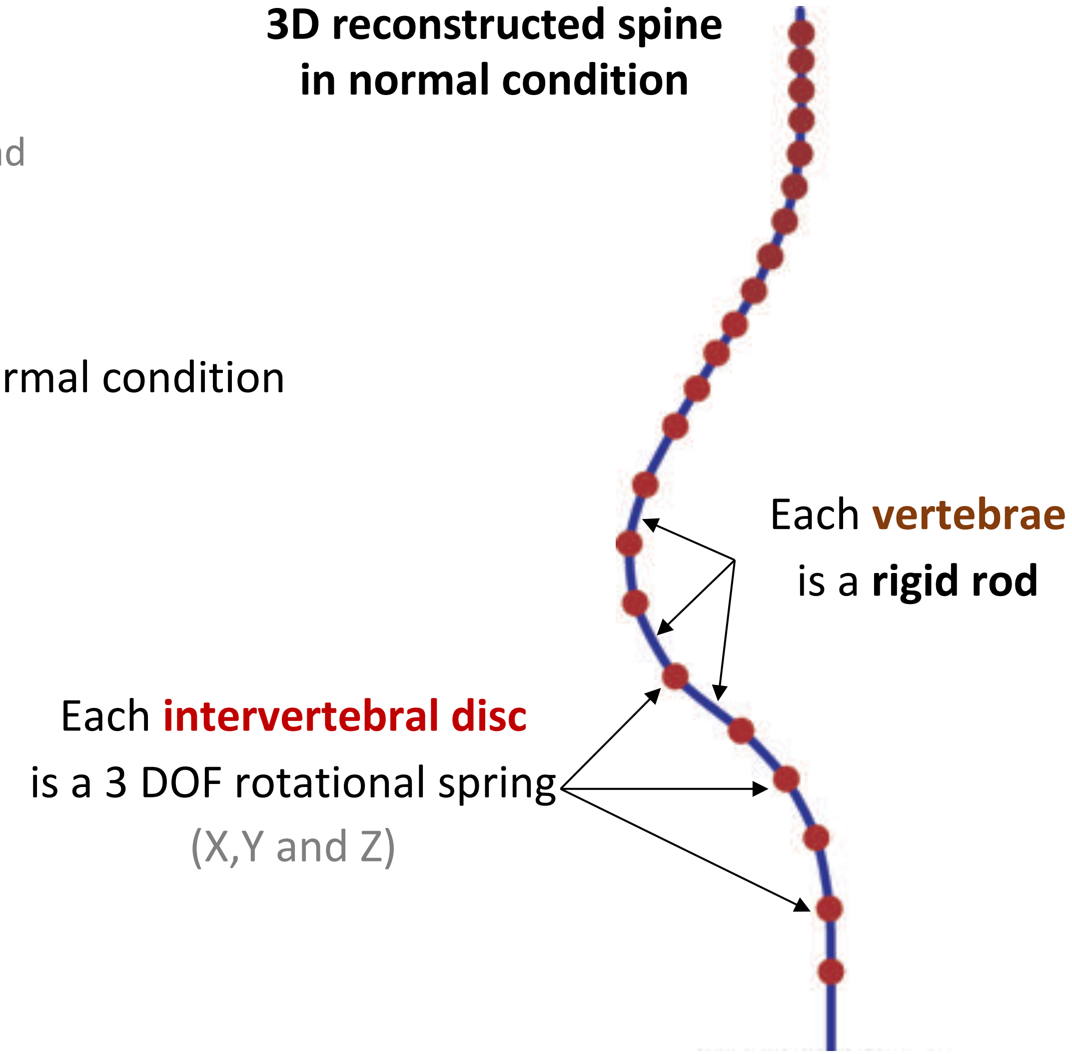

"Beam" FEM Model

1) Experiment

- Apply a load on the spine
- Measure its displacement & the load

2) Model

- Create a FEM of the spine in normal condition
- Add the experimental constrains

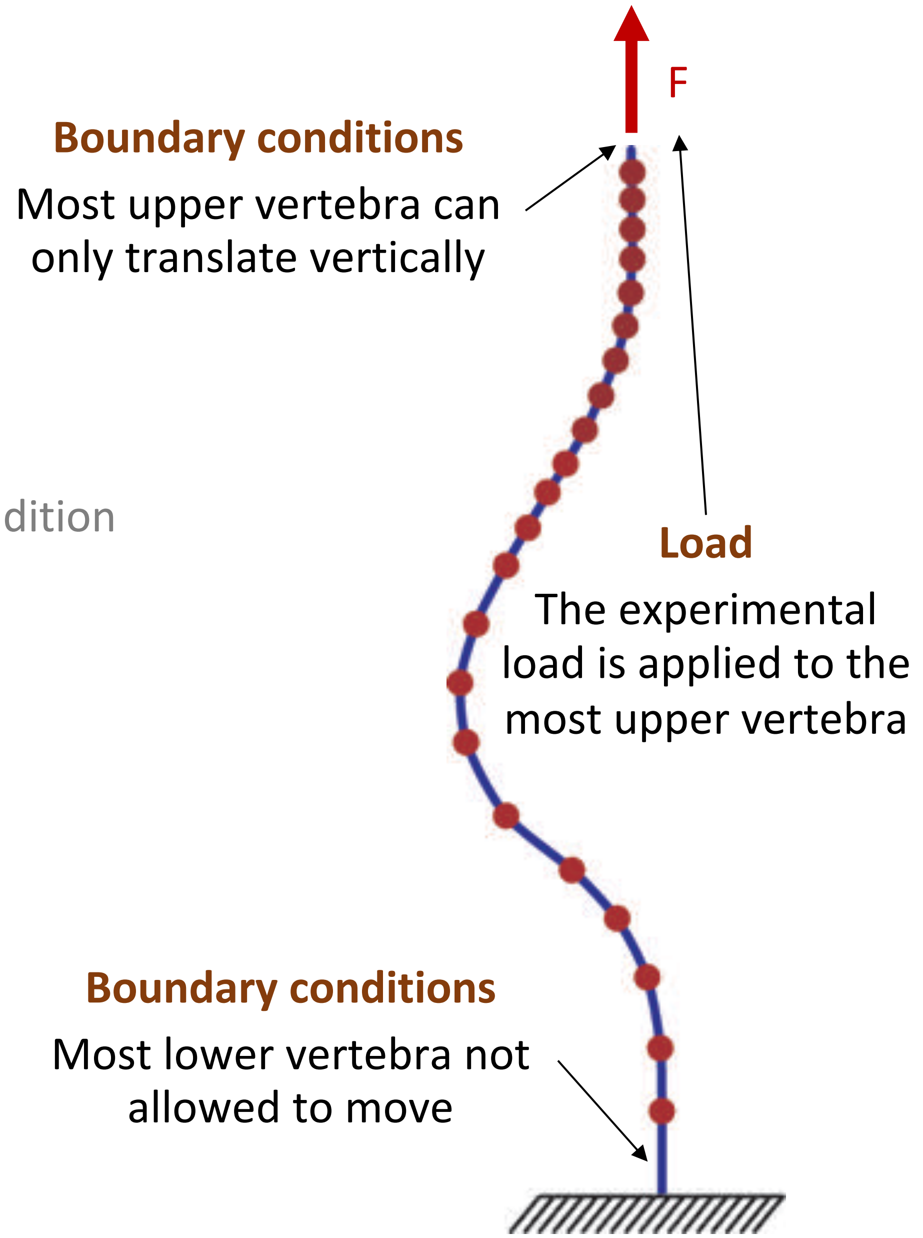

“Beam” FEM Model

1) **Experiment**

- Apply a load on the spine
- Measure its displacement & the load

2) **Model**

- Create a FEM of the spine in normal condition
- Add the experimental constrains
- Set the same stiffness (Kx, Ky, Kz) for every intervertebral disc

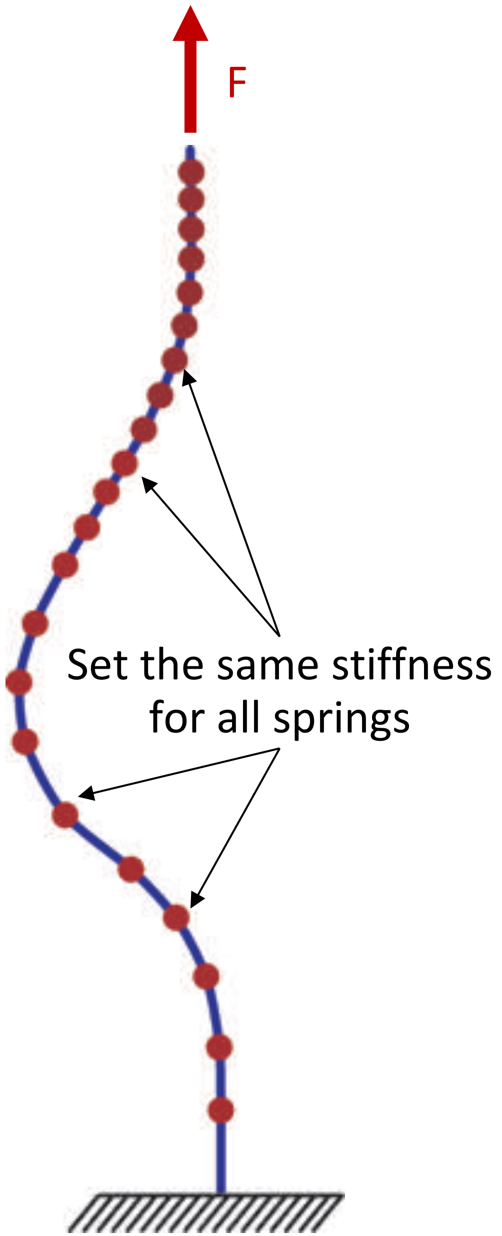

"Beam" FEM Model

1) Experiment

- Choose a subject
- Apply a load on the spine
- Measure its displacement & the load

2) Model

- Create a FEM of the spine in normal condition
- Add the experimental constrains
- Set the (unknown) stiffness of the spine

3) Optimization

- Find the stiffness coefficients (Kx, Ky and Kz) which best explain the experimental displacement.

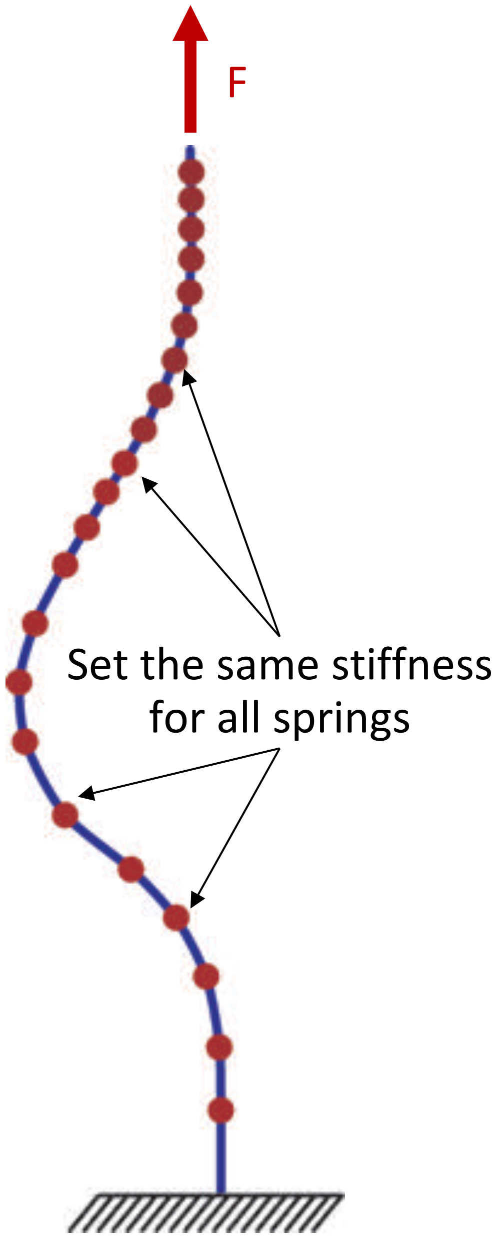

Stiffness optimization

Cost function: $E = \begin{cases} D + P & \text{if } P > 0 \\ D & \text{else} \end{cases}$

- **D is the quality term** (mean distance between the nodes)

$$D = \frac{1}{N} \cdot \sum_{i=1}^{N} \sqrt{(x_i^e - x_i^m)^2 + (y_i^e - y_i^m)^2 + (z_i^e - z_i^m)^2}$$

- **P is the penalty term** (standard deviation of the coefficients should always be smaller than 1 [Nm/deg] *)

$$P = \sqrt{\frac{1}{3} \cdot \sum_{i=1}^{3} (K_i - \overline{K})^2 - S_0}$$

Objective: minimize the cost function

- We use the **Nelder-Mead** optimization algorithm

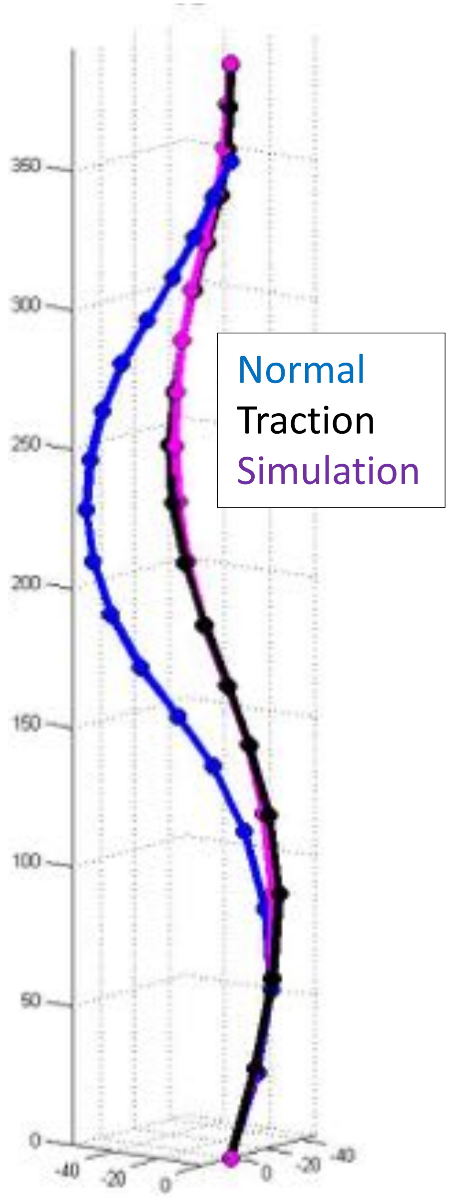

Fitting results

The quality of the fit between 1 and 5 [mm].

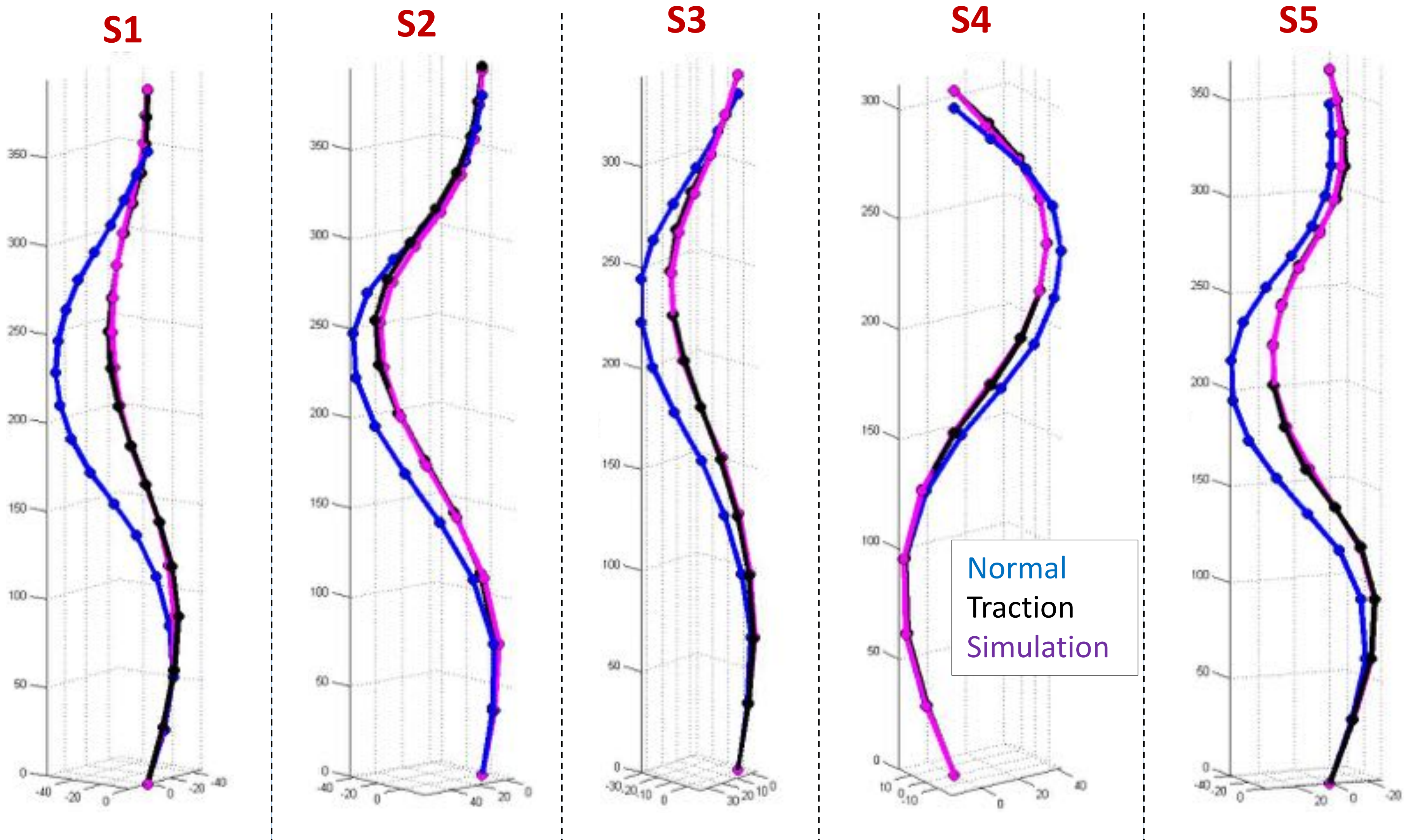

Preoperative Spinal Stiffness

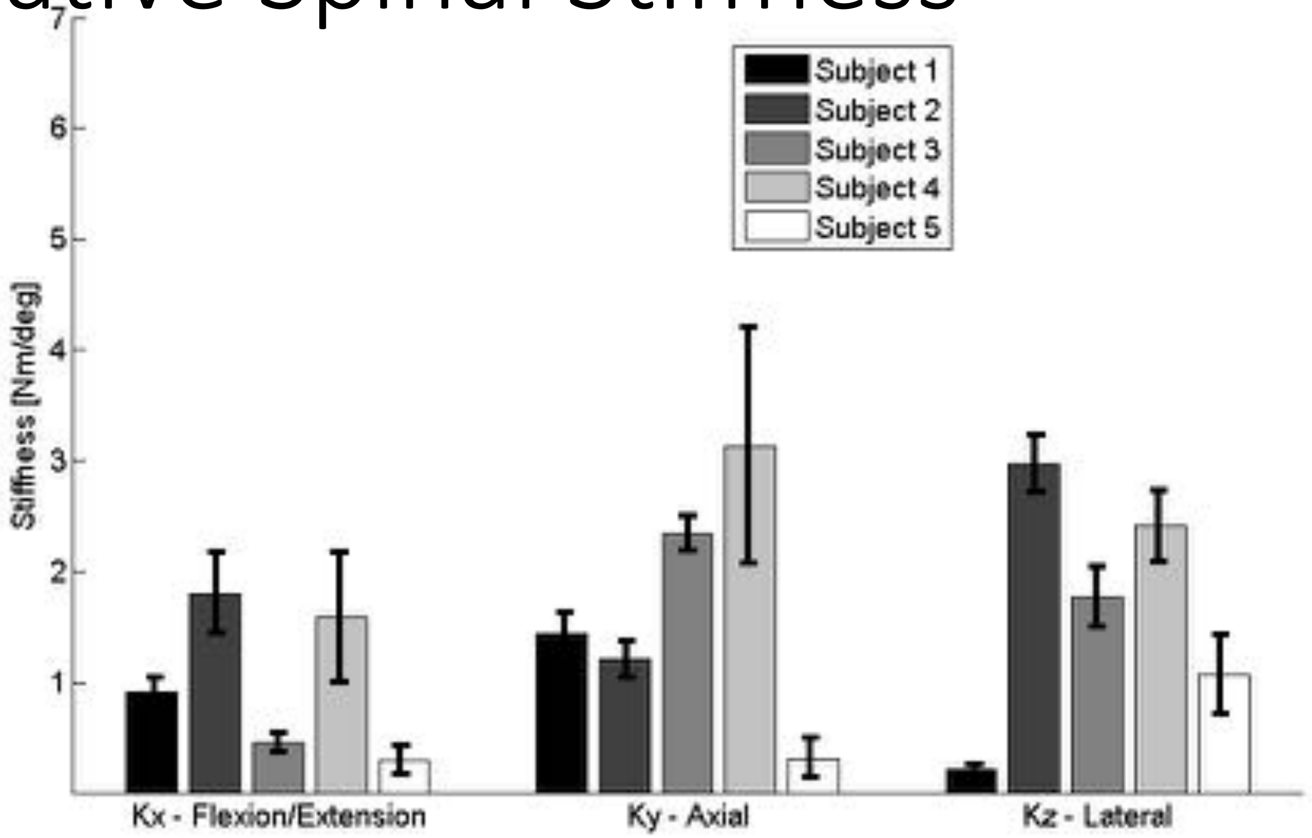

- Large variation in spinal stiffness between patients
- These results emphasizes the patient-specific nature of spinal stiffness

Comparison to intraoperative measurements

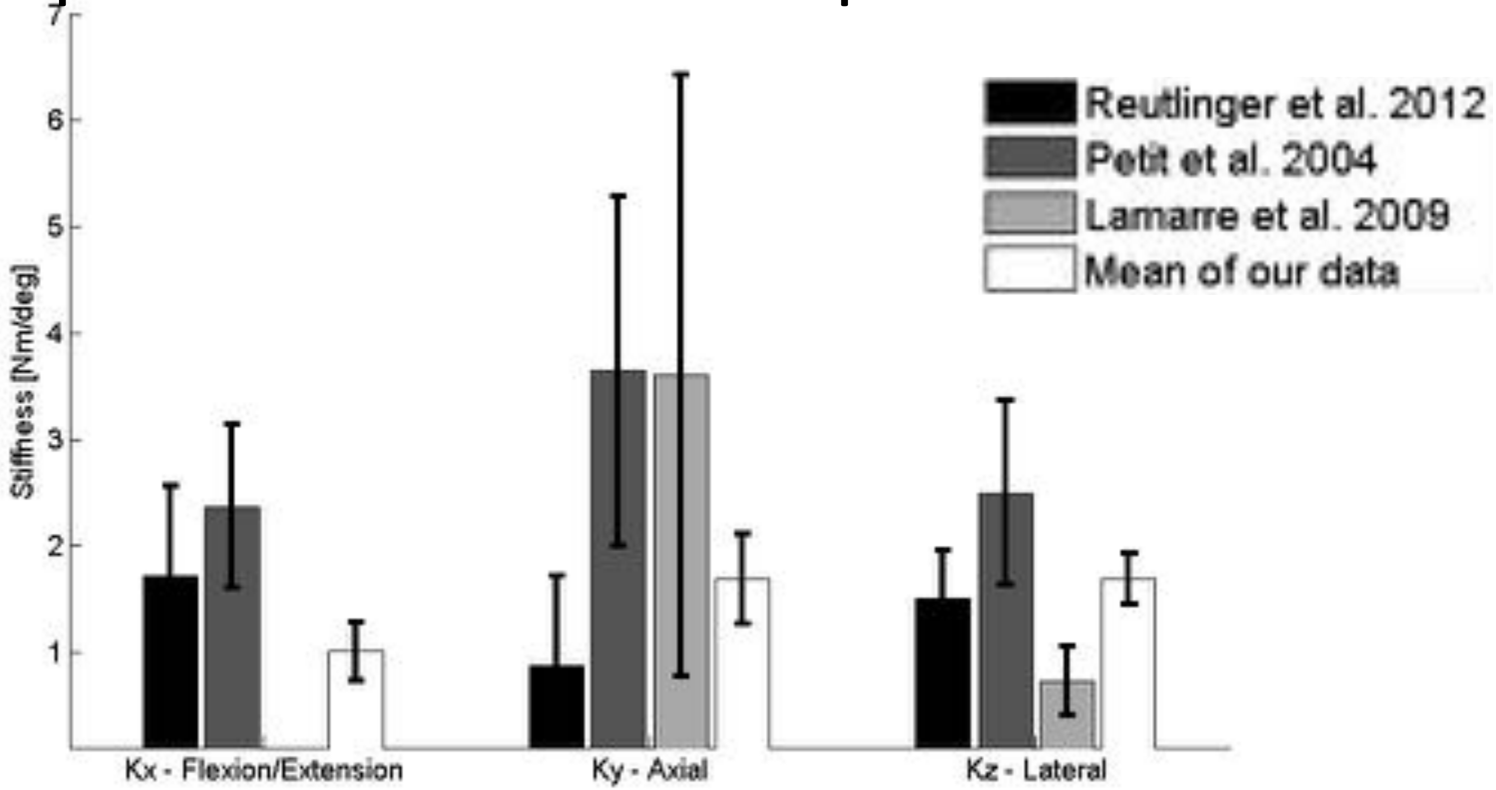

: intra-operative measurement
: side bending test
: suspension test (2D)

- Comparison is hindered by the use of very different clinical tests and different amount of information used to estimate the stiffness
- Our results falls within 1 STD of previous intraoperative measurements

Summary

UNIVERSITÄT BERN

- Personalized mechanical simulations
  - Patient's anatomy
  - Obtain mechanical characteristics in-vivo (intra-operative or pre-operative)
  - Loading !?
- Identification of material parameters using inverse FE techniques
- Virtual test bench
  - For development of surgical tools / implants
  - Personalization of the surgical procedure

SpineBot

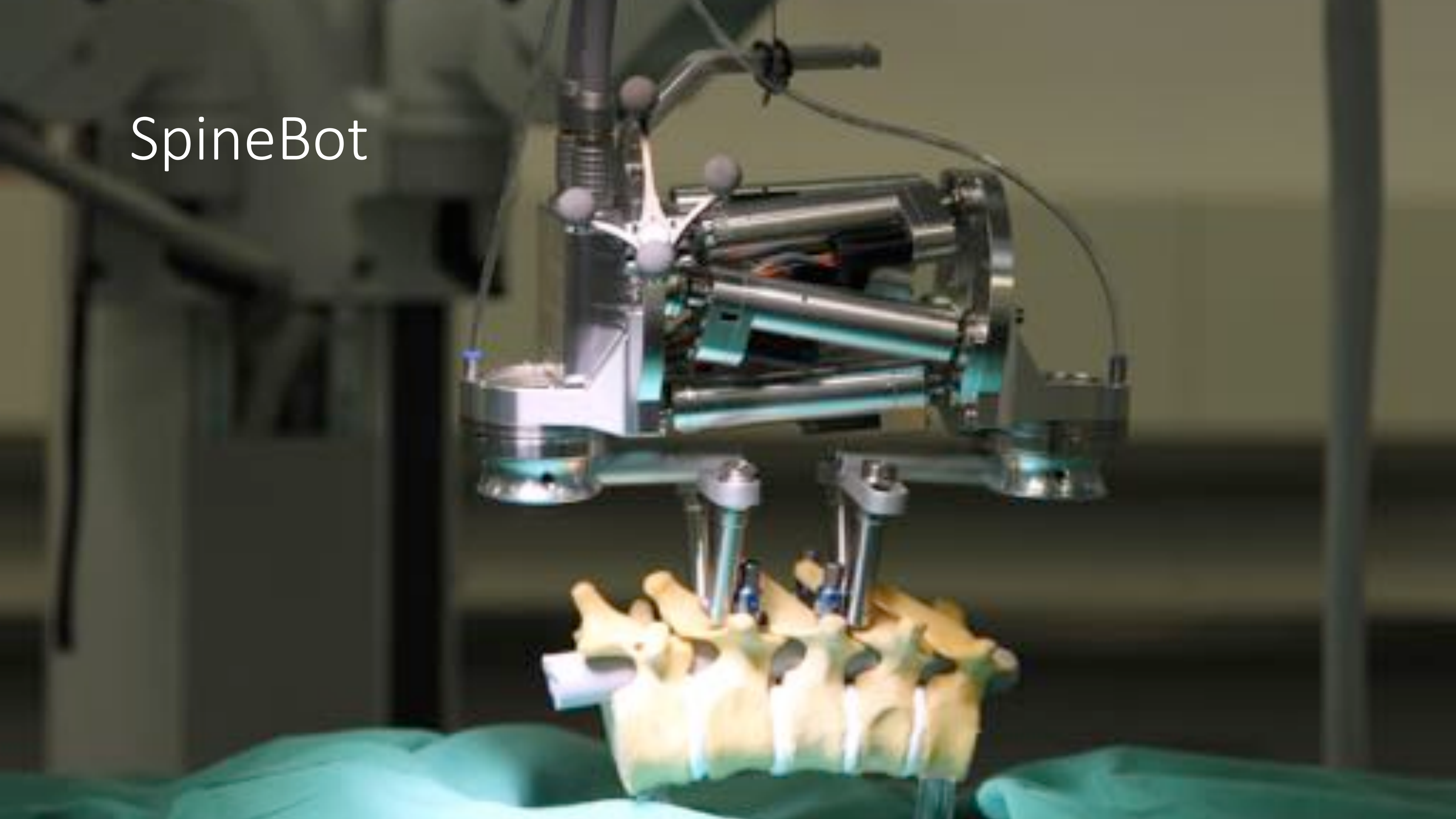

SpineBot

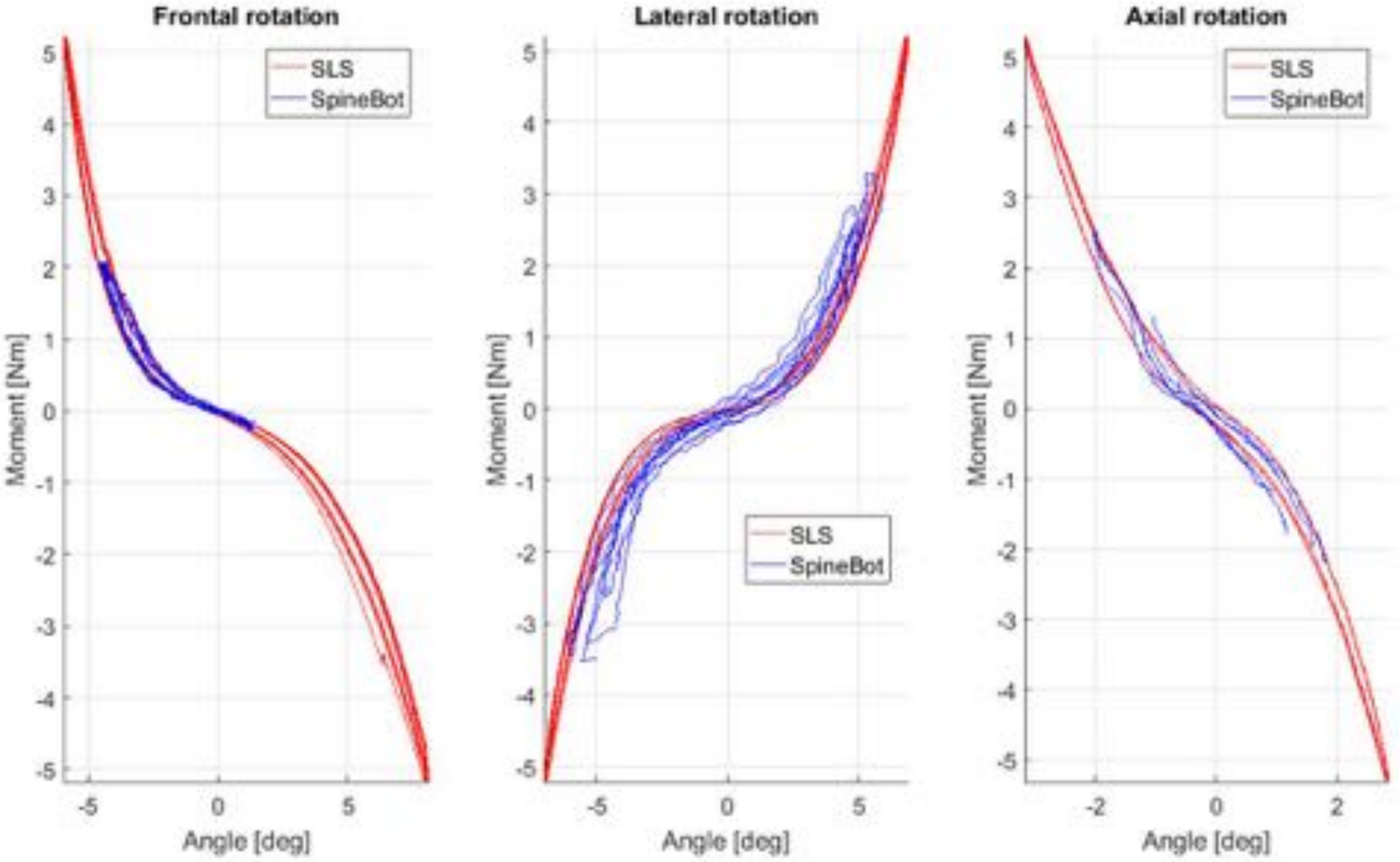
Frontal rotation
SLS
SpineBot
Moment [Nm]
Angle [deg]
Lateral rotation
SLS
SpineBot
Moment [Nm]
Angle [deg]
Axial rotation
SLS
SpineBot
Moment [Nm]
Angle [deg]

Optimeyes^{TM}

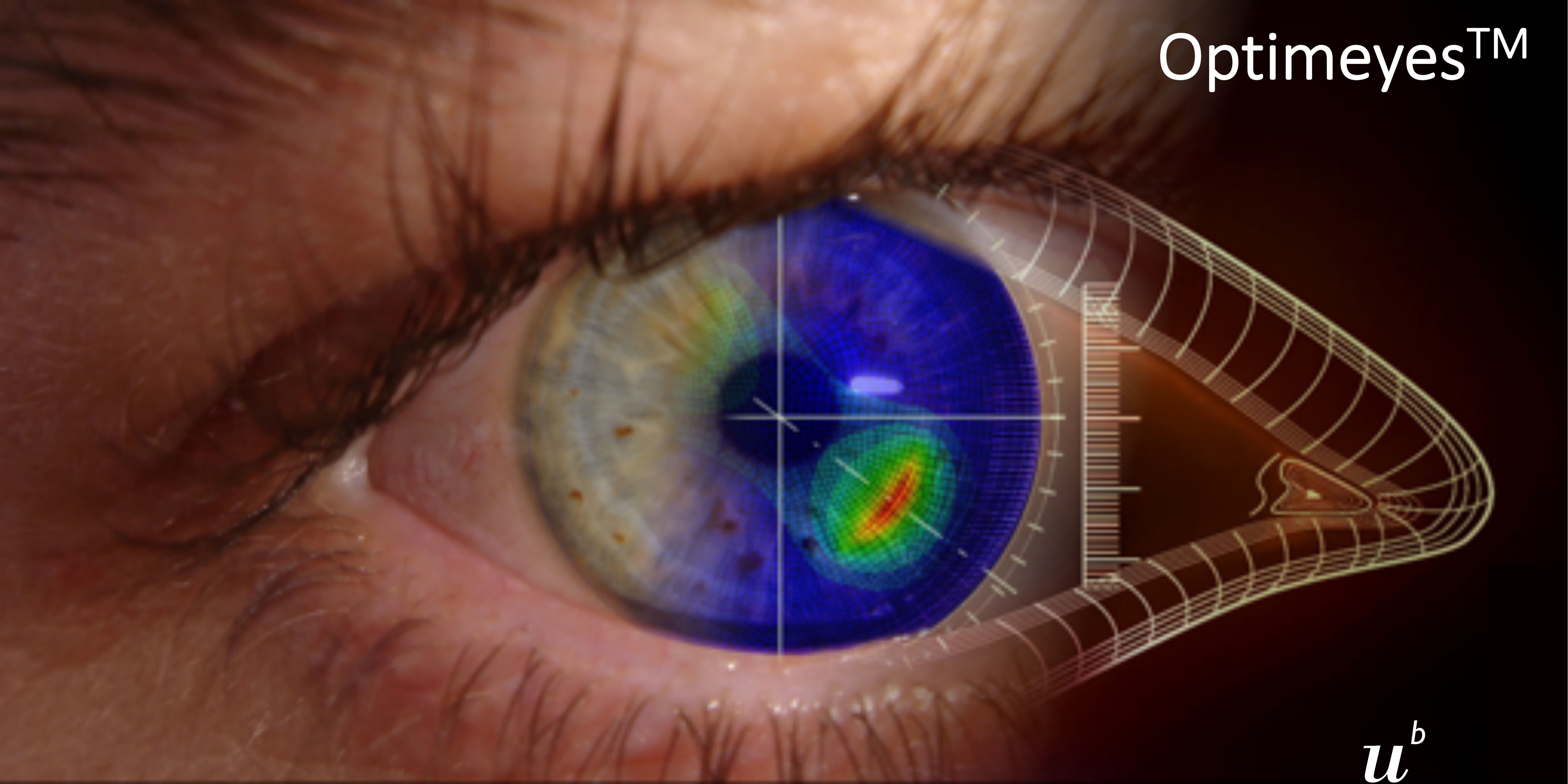

Optimeyes ANSYS

UNIVERSITÄT BERN

Introduction

- 51% of the world population is presbyopic
- Solution: intracorneal lens (ICL)
  - Minimally invasive
  - Reversible method
- Potential problems:
  - Asymmetric cut may induce optical aberrations
  - An intra-corneal implant may act as a barrier for nutrients

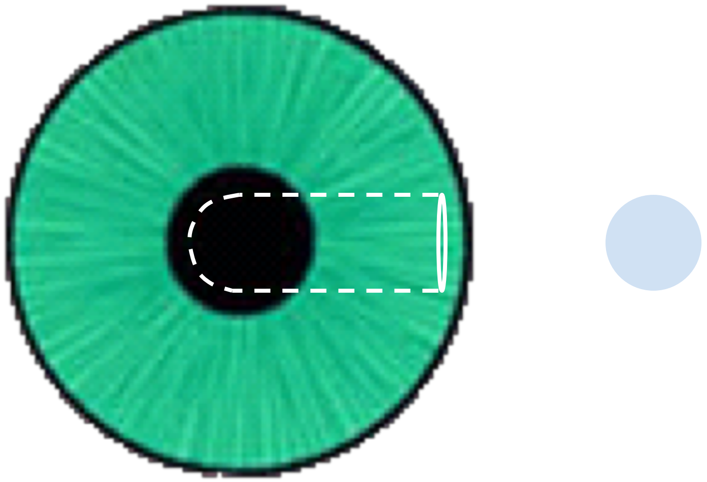

The cornea is an avascular tissue

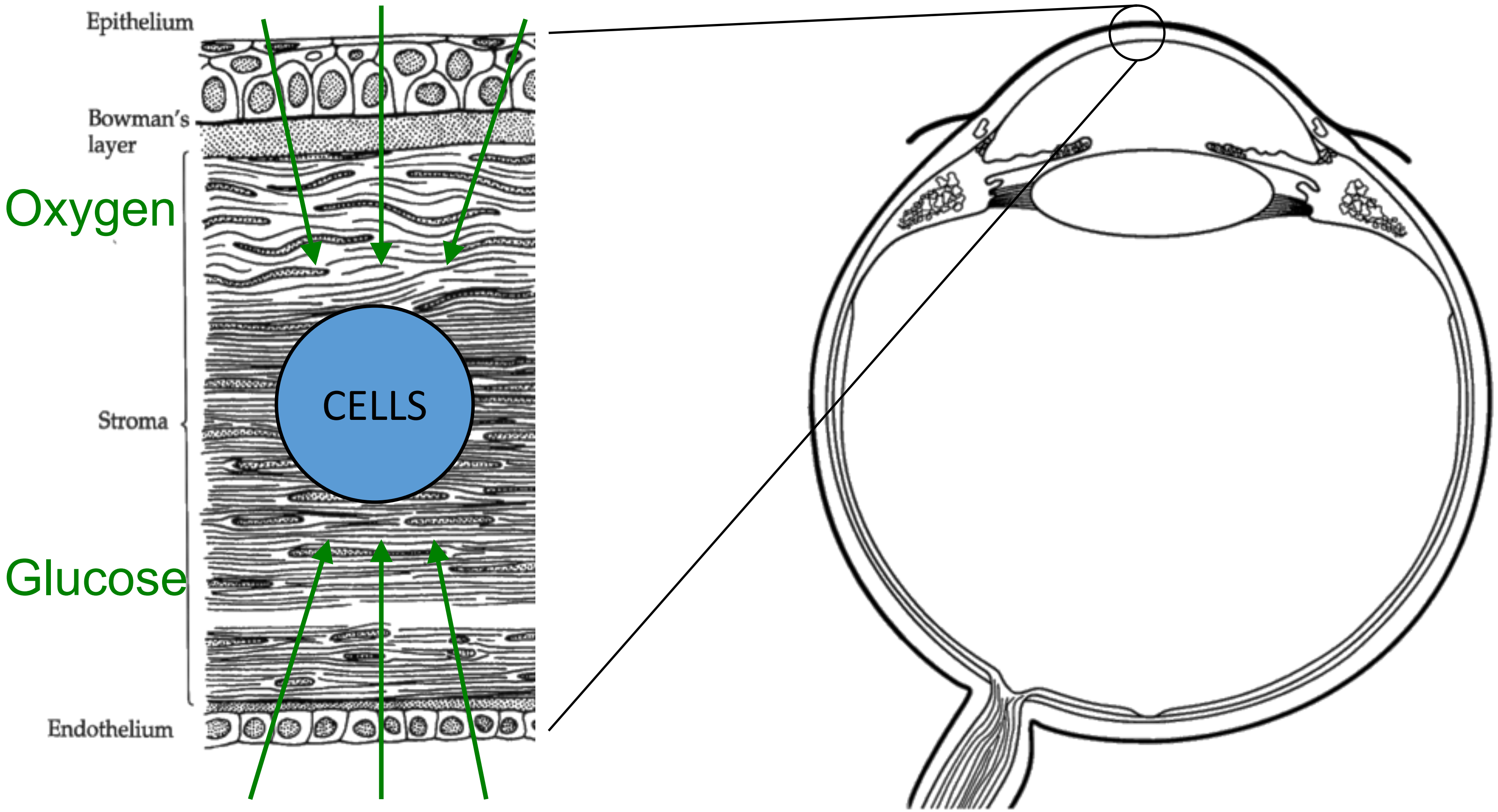

Nutrients and waste products diffuse through the tissue

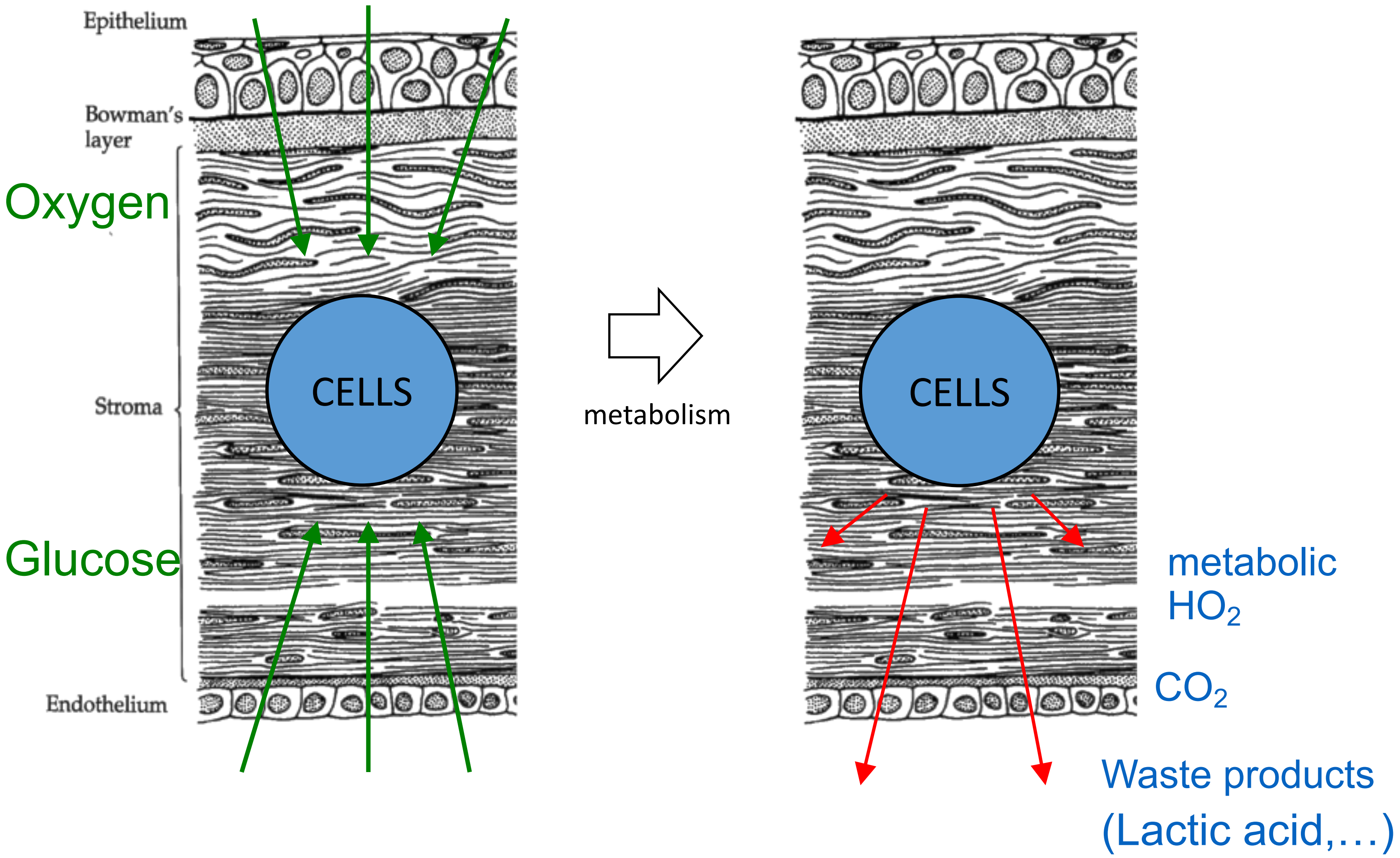

Impermeable contact lens wear

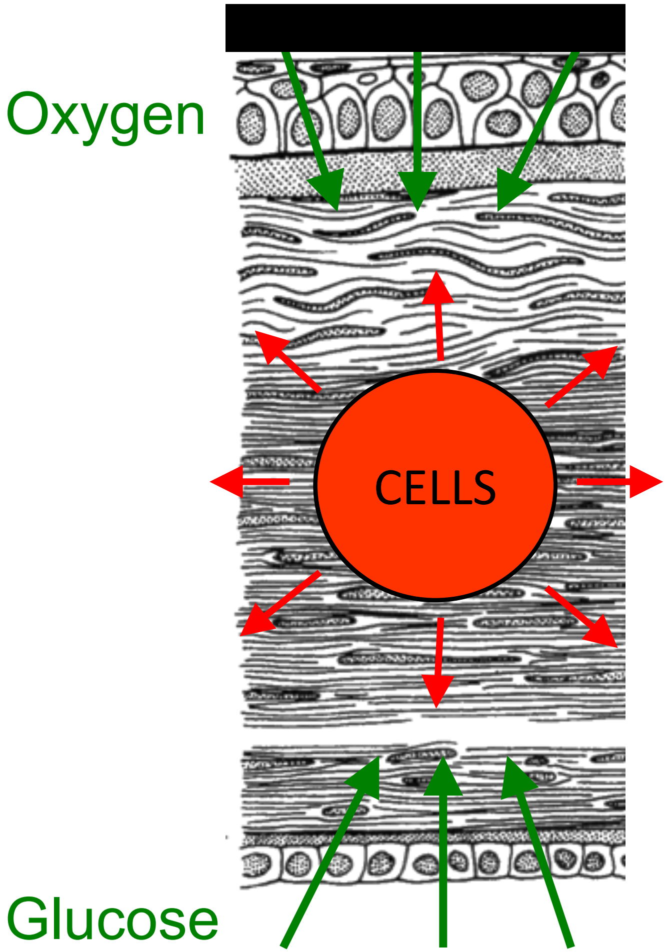

- Contact lens blocks O_2 supply
- Anaerobic cell metabolism
- Increase in Lactate concentration
  - Edema[1,2]
  - Foggy vision[1,2]
  - Tissue acidosis
  - …

1. Klyce, 1981
2. Riley, 1972

Intracorneal lens ?

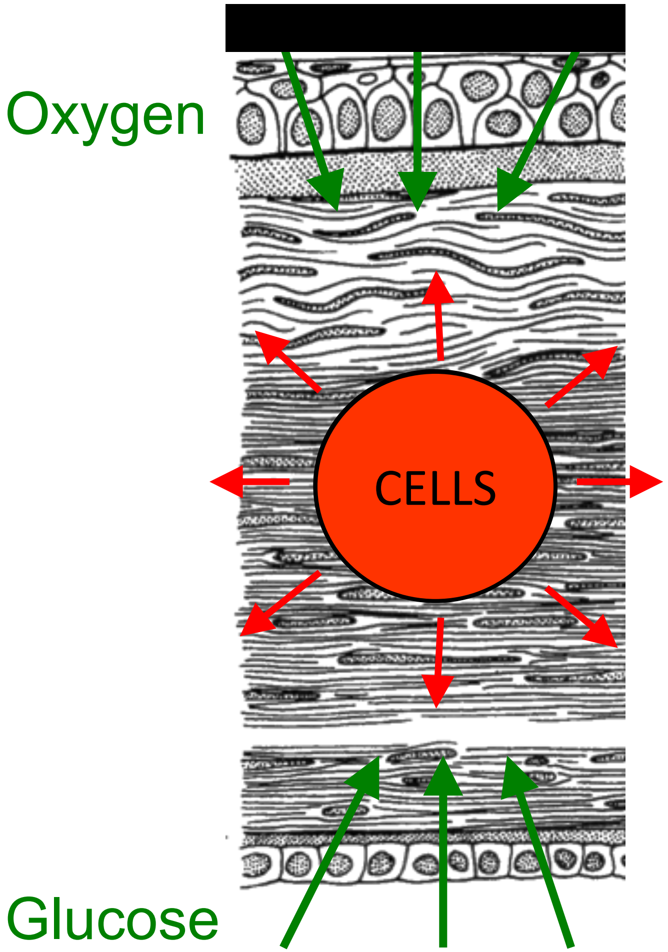

Objective

Address nutrient transport in the cornea after ICL implantation by computer simulations

Geometry / boundaries

Axisymetric finite element model of the cornea:

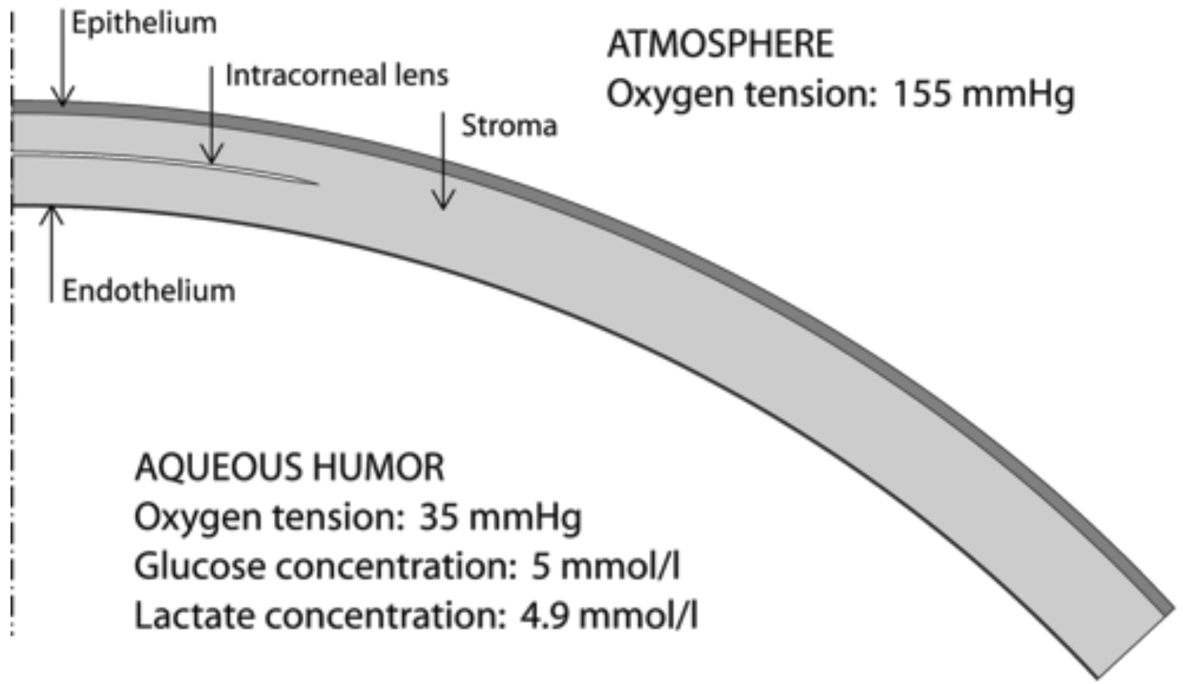

FE model, nutrient transport in the cornea

- Diffusion equation:

$$\nabla\left(D\cdot\nabla C^{\alpha}\right)+q^{\alpha}=\frac{\partial C^{\alpha}}{\partial t}$$

Consumption

α: oxygen, glucose

- Parametric lens diffusivity:

$$D_{lens}=\beta\cdot D_{stroma}$$

β : 0, 10^{-3}, 10^{-2}, 10^{-1}, 1

- Different layer and species consumption rates:

$$q^{\alpha}=f(c^{\alpha})$$

Cell’s nutrient consumption rate depend on solute availability

$$q^{\alpha} = f(c^{\alpha})$$

Oxygen

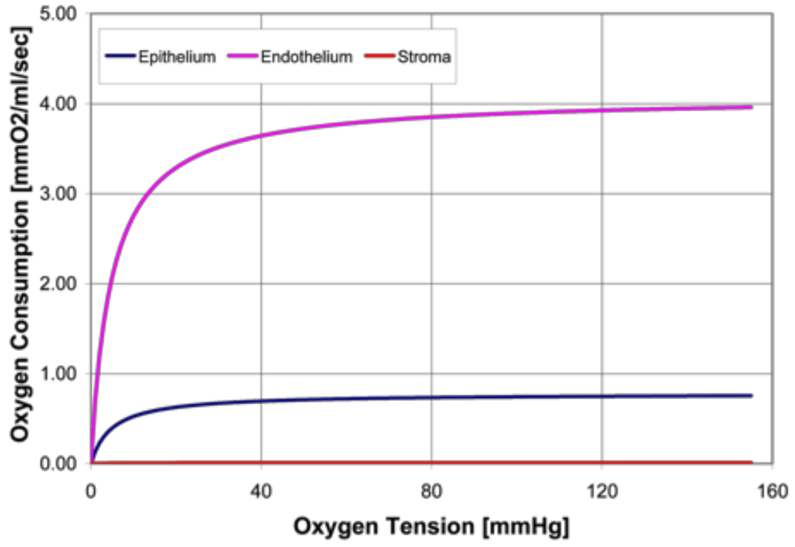

[1]Freeman, 1972, *J. of Physiol.*

[2]Jauregui & Fatt, 1972, *Am.J.Optom.Arch.Am.Acad.Optom*.

Glucose

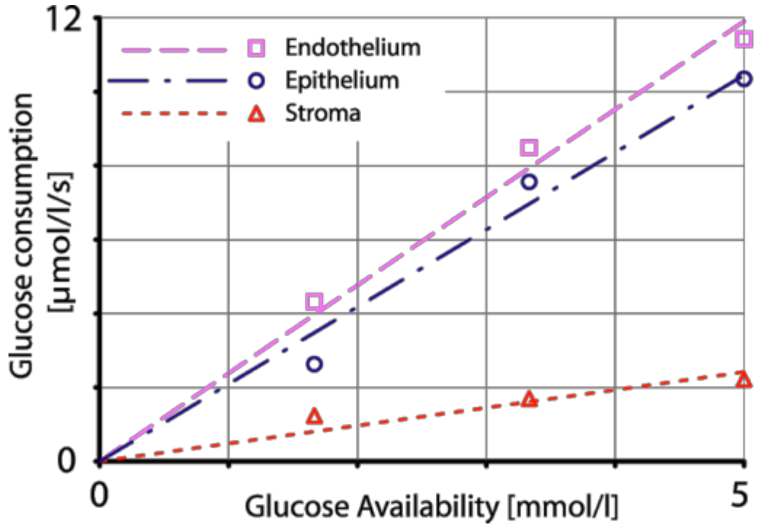

[3]Zurawski et al., 1989, *Curr Eye Res.*

Consumption/diffusivity on humans

UNIVERSITÄT BERN

- Current mathematical models are based on consumption and diffusivity measured in-vitro in rabbit corneas
- Bonnano[1] measured oxygen tension under a contact lens non-invasively on humans
    - Recorded oxygen tension after 5 minute eye closure with three different lenses

1. Bonanno et al. 2002

Results, transient response

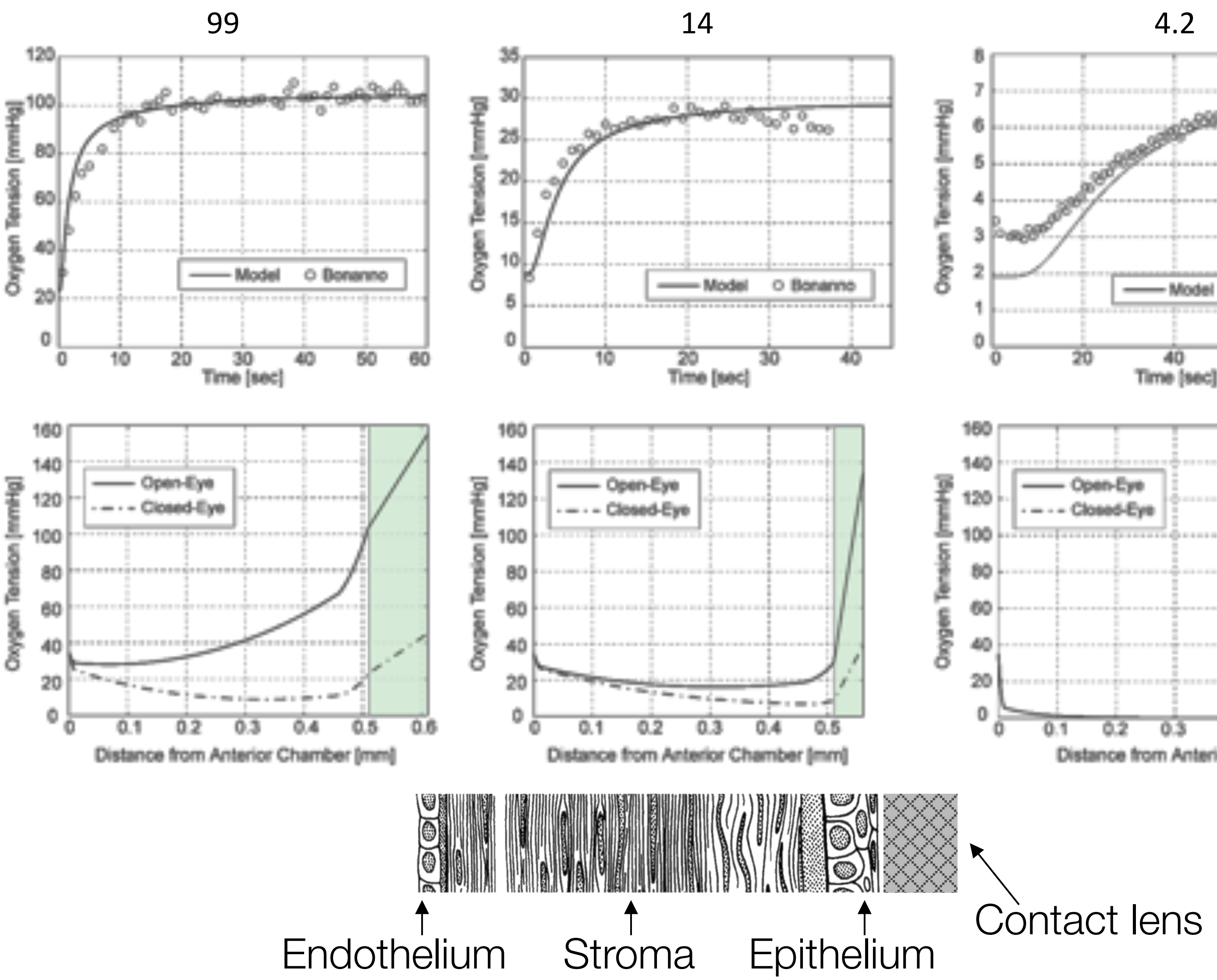

In vivo oxygen diffusivity and consumption

UNIVERSITÄT BERN

	Present model (human)		Fatt *et al.* (rabbit)		Ratio
q*	$5.75\ 10^{-5}$	$mlO_2/ml/s$	$2.24\ 10^{-5}$	$mlO_2/ml/s$	**2.5**
Dk	86.2	Barrer	30	Barrer	**2.9**

q*: consumption rate at saturate oxygen tension

k : Henry's solubility constant (nmol / mm^3 / mmHg)

O_2 permeability in Barrer = 10^{-11} (cm^2 mlO^2 / s / cm^3/mmHg)

What is the best position for an ICL ?

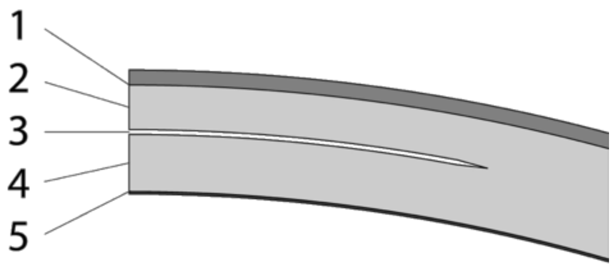

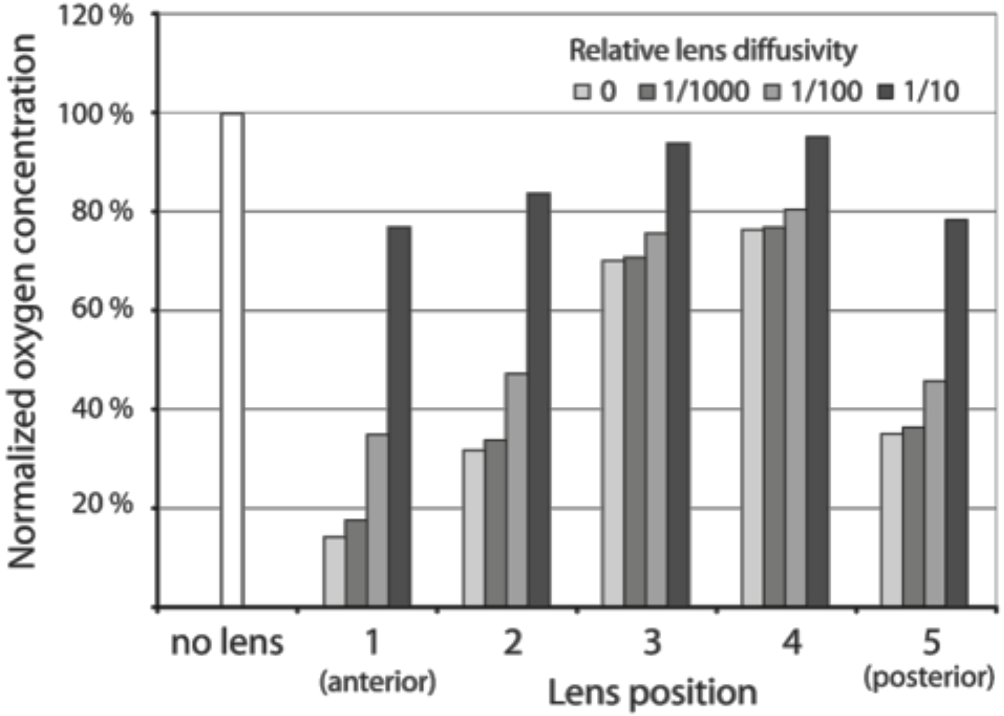

> Better oxygen supply at mid-posterior stroma

What is the influence of lens diffusivity on nutrient distribution ?

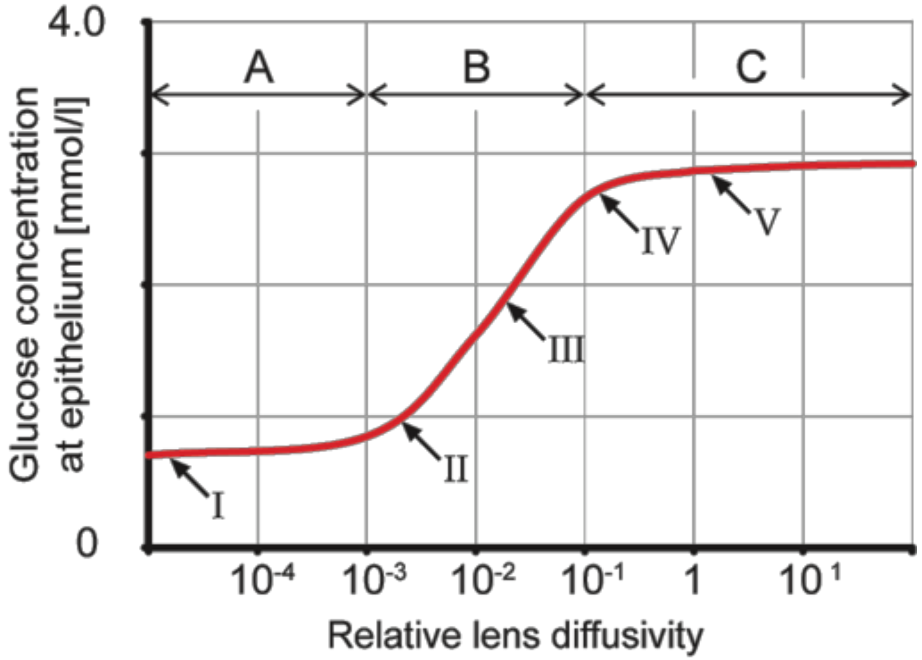

I. PMMA
II. 25% Hydrogel
III. 50% Hydrogel
IV. 75% Hydrogel
V. PFTE

> Transition zone around relative lens diffusivity of 1/100

Summary

> Possible to calculate nutrient transport using simple heat transfer solver (could be extended to growth modulation algorithms)

> Major challenge concerns the proper model parameters
  - Diffusivity & consumption from invivo measurements
  - Limited to healthy metabolism
  - No data available to quantify the metabolic activities for different level of O2, Glucose and lactic acid

> Optimal depth position (~3/4 corneal thickness) and show no depletion of nutrients with intracorneal rings

> Nutrient pathway changes around 1/100 lens diffusivity

> Mechanical deformation of the cornea not included
  - Effect of the cut
  - Stiffening due to the lens

The human eye

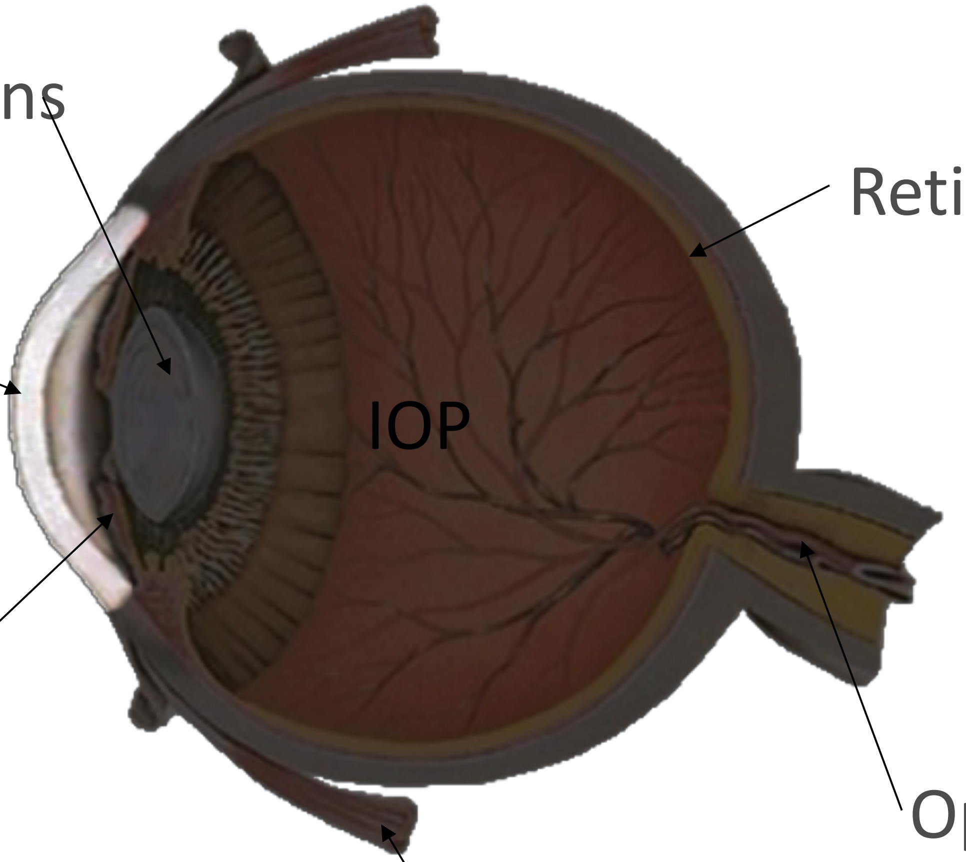

Refractive power

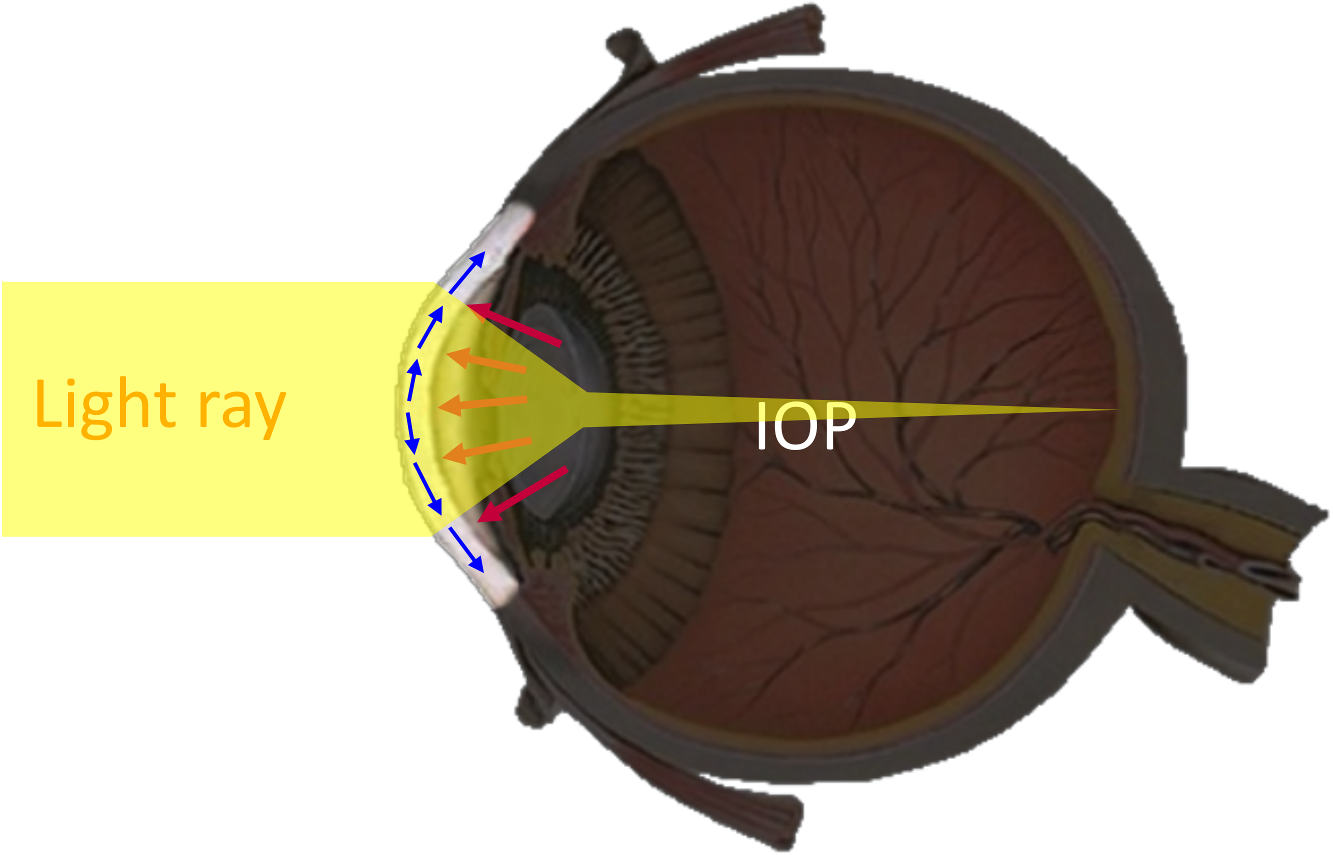

Cornea contributes ~2/3 of refractive power to our eyes

Planning ophthalmic interventions

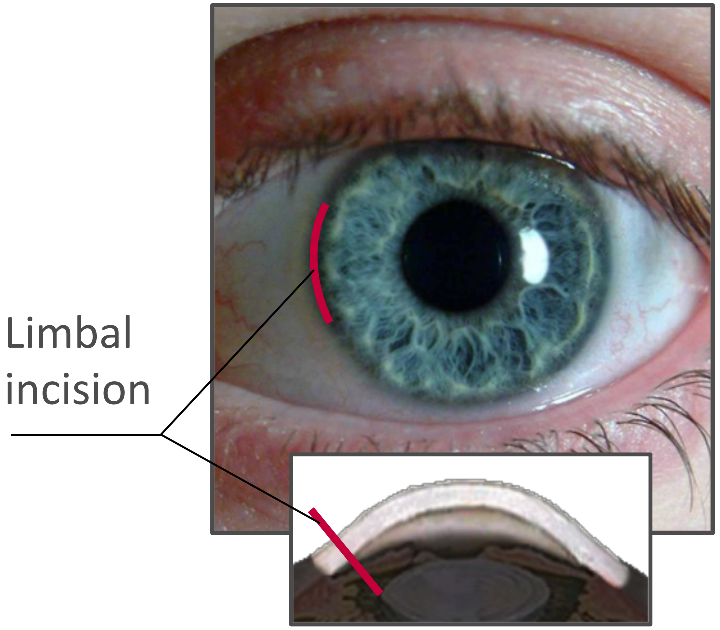

Cataract surgery

- Incision in the limbus changes astigmatism
- Over 2'500'000 surgeries a year in the US

LASER ablating tissue

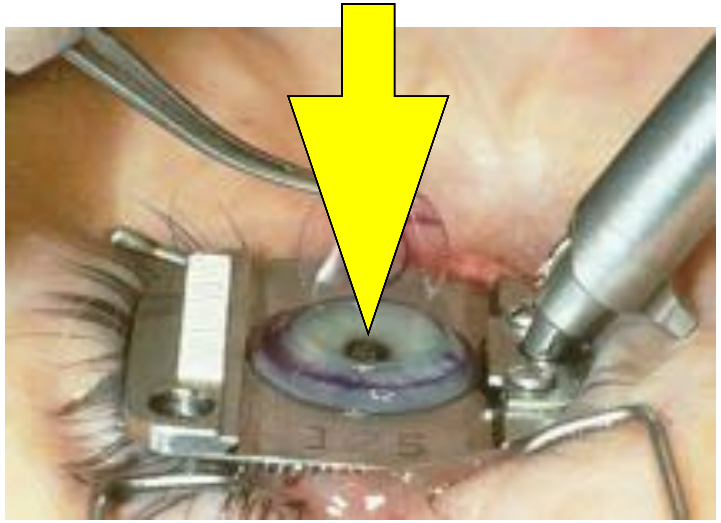

Refractive surgery (LASIK)

- Cutting tissue over the refractive zone
- Thinning the structure by vaporizing tissue
- Over 1'000'000 surgeries per year

Material model

Penalty to prevent volume change:

$$\Psi = U[J] + \overline{\Psi}[\overline{C}] + \frac{1}{\pi}\int \Phi(R,\varphi;\theta)(\overline{\Psi}_{f1}[\overline{C},A] + \overline{\Psi}_{f2}[\overline{C},B])d\theta$$

Tissue features modeled:

- Incompressibility

Material model

Neo-hookean material as tissue matrix:

$$\Psi = U[J] + \overline{\Psi}[\overline{C}] + \frac{1}{\pi}\int \Phi(R,\varphi;\theta)(\overline{\Psi}_{f1}[\overline{C},A] + \overline{\Psi}_{f2}[\overline{C},B])d\theta$$

Tissue features modeled:

- Incompressibility
- Isotropic tissue matrix (Proteoglycans, Glycosaminoglycans …)

Material model

Ogden material for collagen fibers:

$$\Psi = U[J \ldots {}_2[\overline{C}, B])d\theta$$

Tissue features r

- Incompressibil
- Isotropic tissue Glycosaminogl
- Main collagen

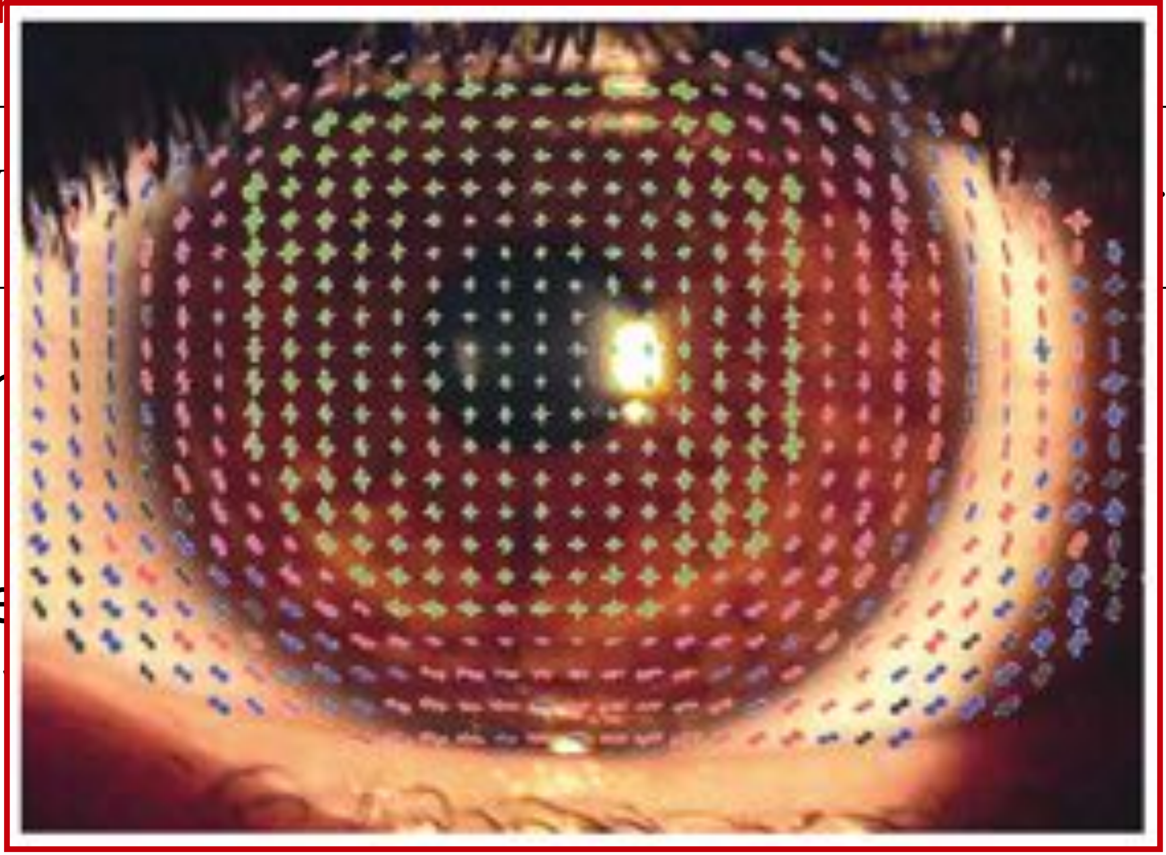

Source: Aghamohammadzadeh et. al. (2004)

Material model

Ogden material for collagen cross-links:

$$\Psi = U[J] + \overline{\Psi}[\overline{C}] + \frac{1}{\pi}\int \Phi(R,\varphi;\theta)(\overline{\Psi}_{f1}[\overline{C},A] + \overline{\Psi}_{f2}[\overline{C},B])d\theta$$

Tissue features modeled:

- Incompressibility
- Isotropic tissue matrix (Proteoglycans, Glycosaminoglycans …)
- Main collagen fibers with realistic distribution
- Collagen cross-links

UNIVERSITÄT BERN

Identification of mechanical parameters

> Experimental data:

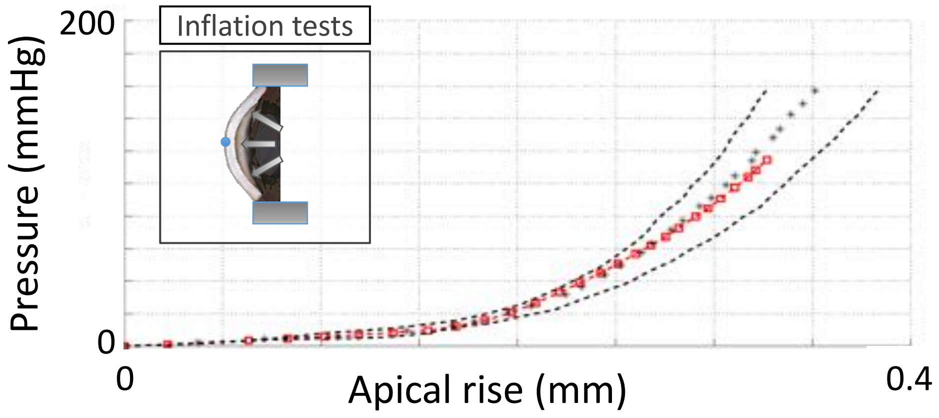

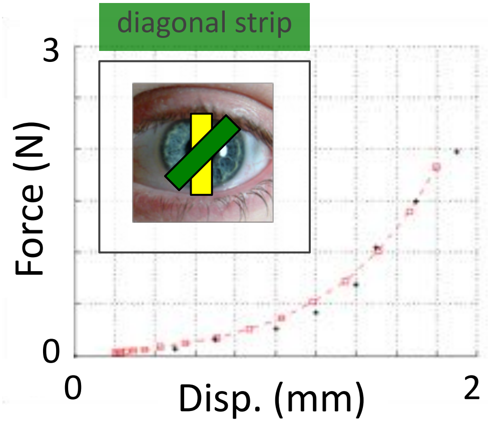

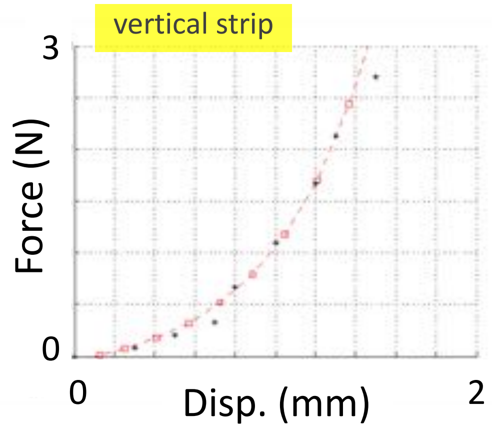

> Identified parameters

Increased cross-links | **Elasticity loss**

	C_{10} [MPa]	γ_{f1}	μ_{f1} [MPa]	γ_{f2}	μ_{f2} [MPa]	λ_{crimp}
65-79y	0.06	0.13	24.00	0.08	95.00	1.5%
80-95y	0.06	0.11	25.81	0.13	78.51	1.1%
	Matrix	Main fibers		Cross-links		Crimp

Patient-specific models

UNIVERSITÄT
BERN

1. FE model able to represent surgical intervention

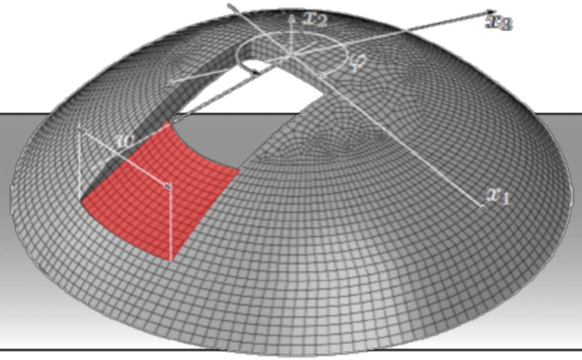

2. FE model matching patients' topography

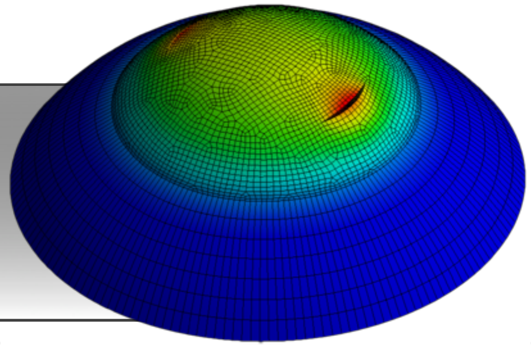

3. Validation on refractive interventions

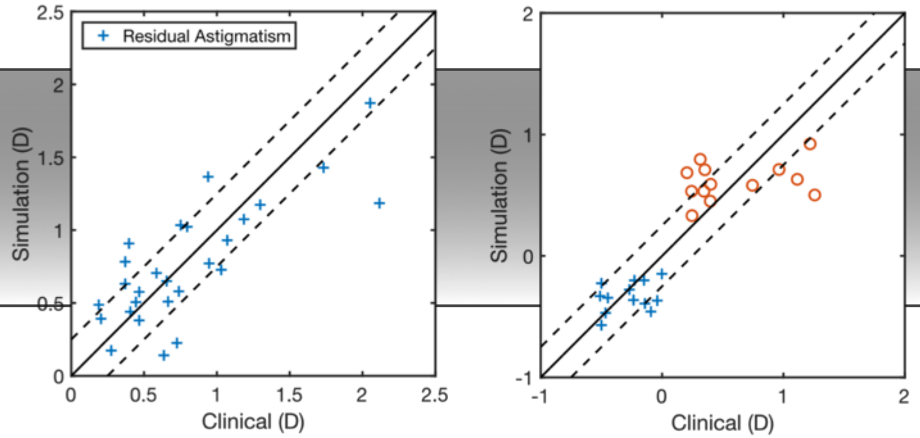

UNIVERSITÄT BERN

Clinical validation

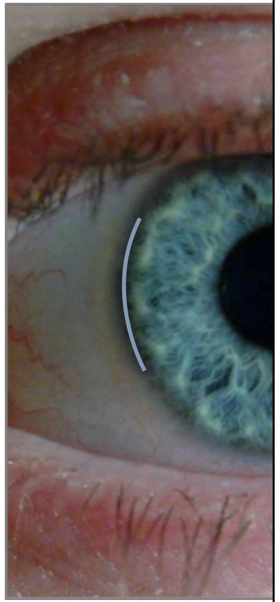

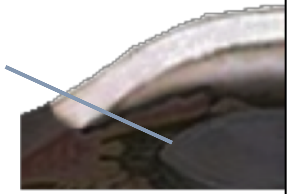

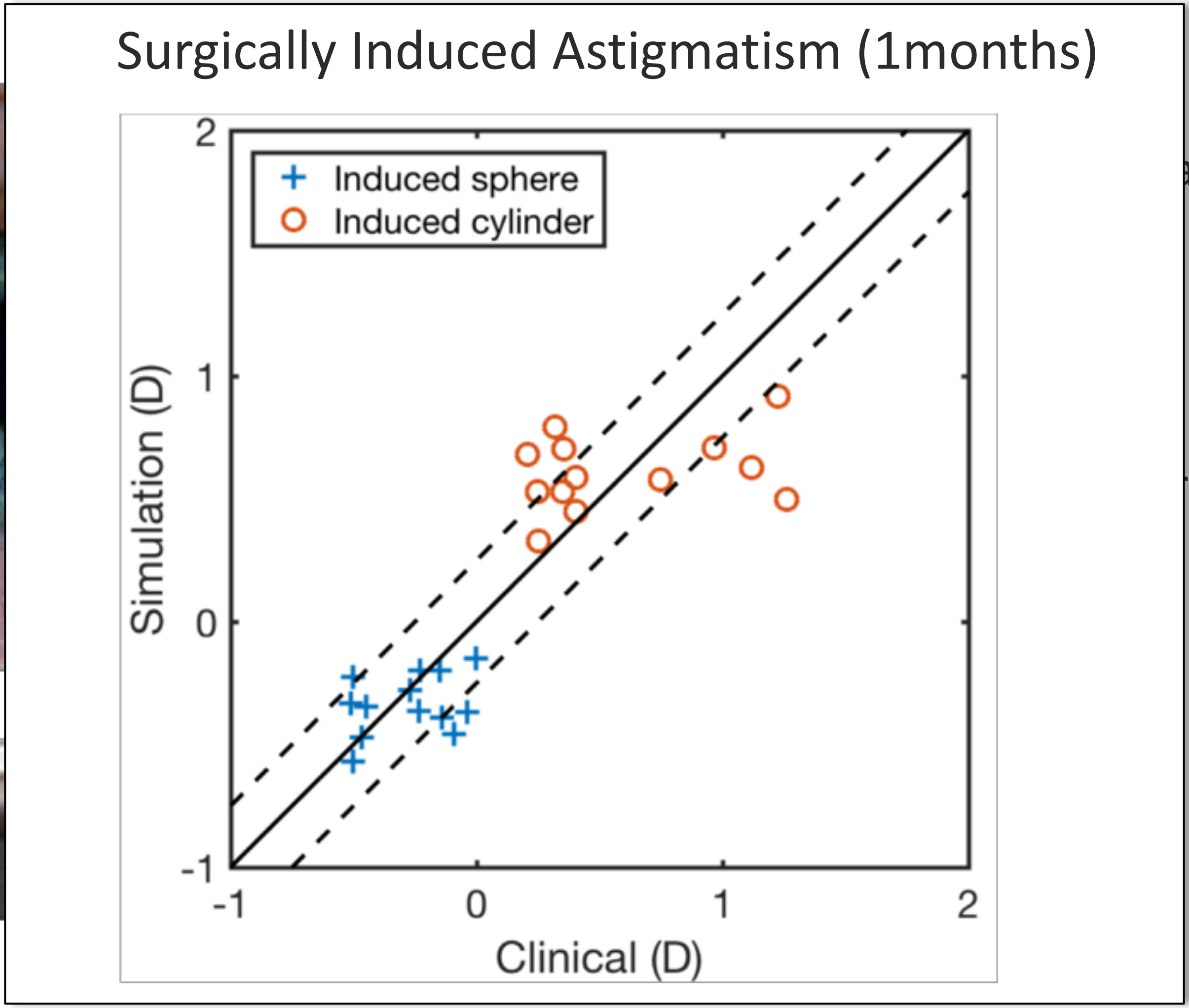

l study

hy measurement

patient (1x pre and

Software tool: OptimEyes

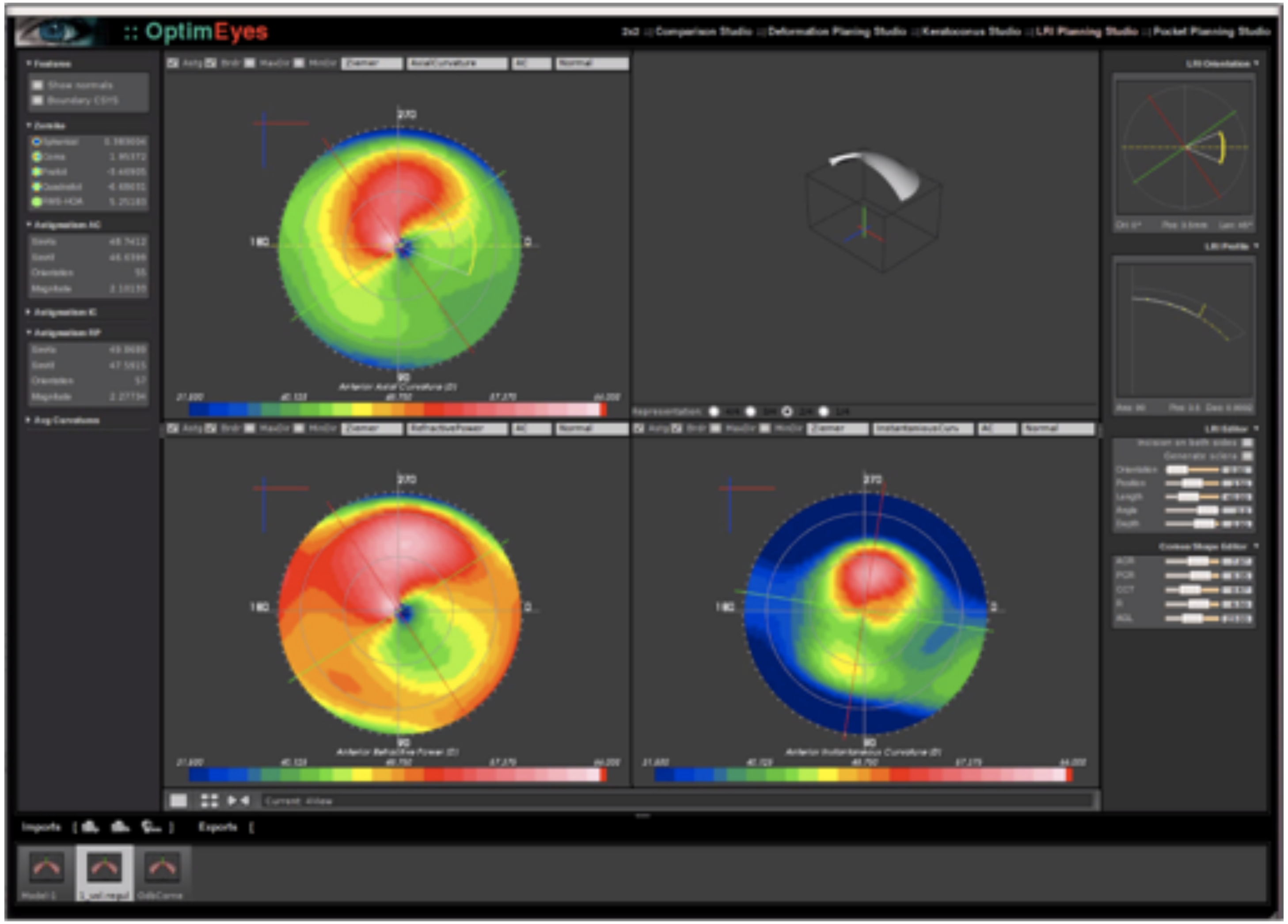

Optimization of astigmatism

Arcuate keratotomy

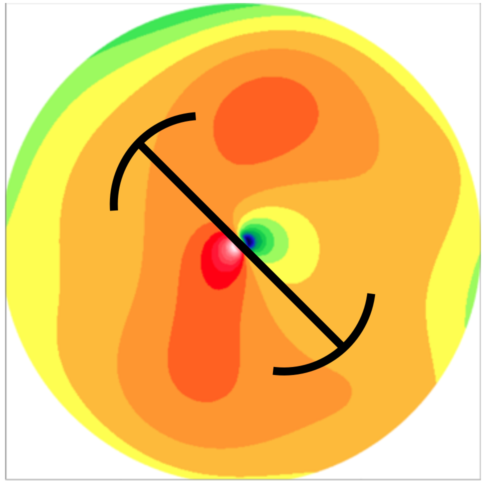

- Position: 3.5 - 5.5 mm
- Opening: 20° - 75°
- Depth: 0.2 - 0.9

Pre-op. – Astigmatism of 5.5 D

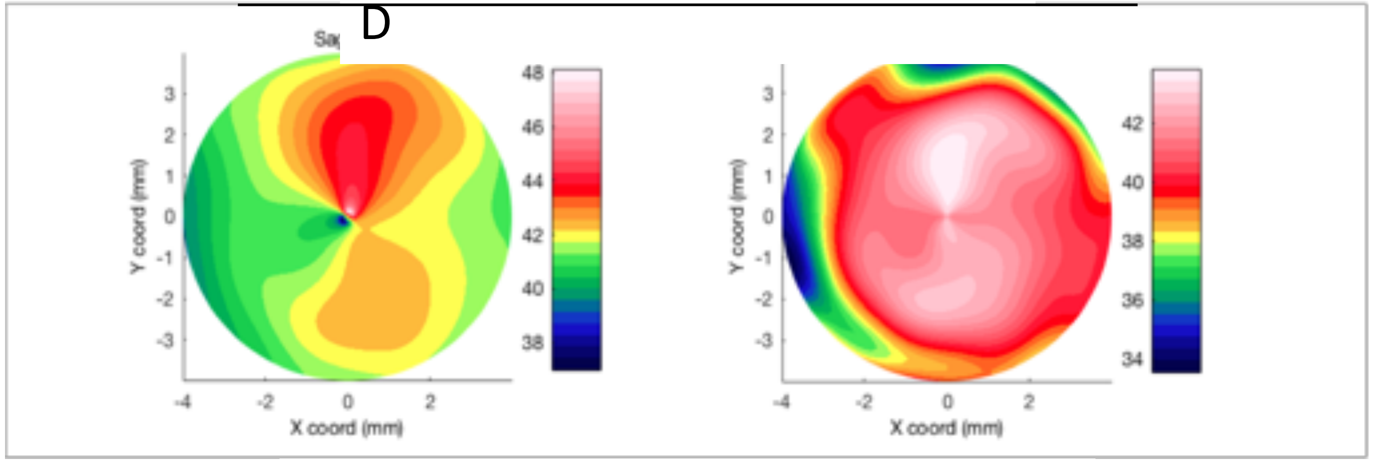

Post-op. – Astigmatism of 0.007 D

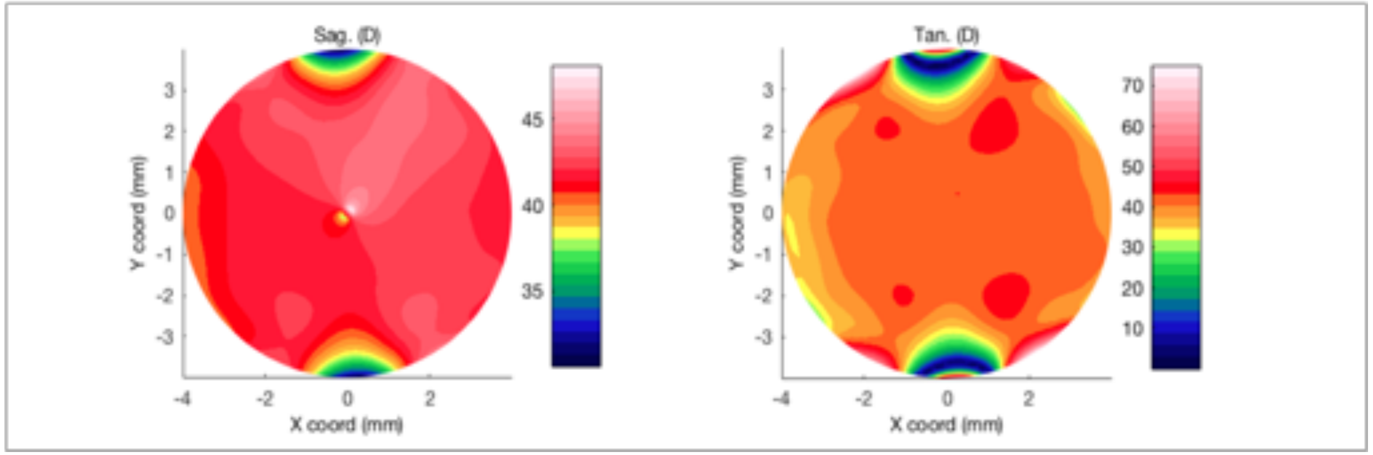

Patient-specific optimization more accurate than nomogram (~ 700 patients)

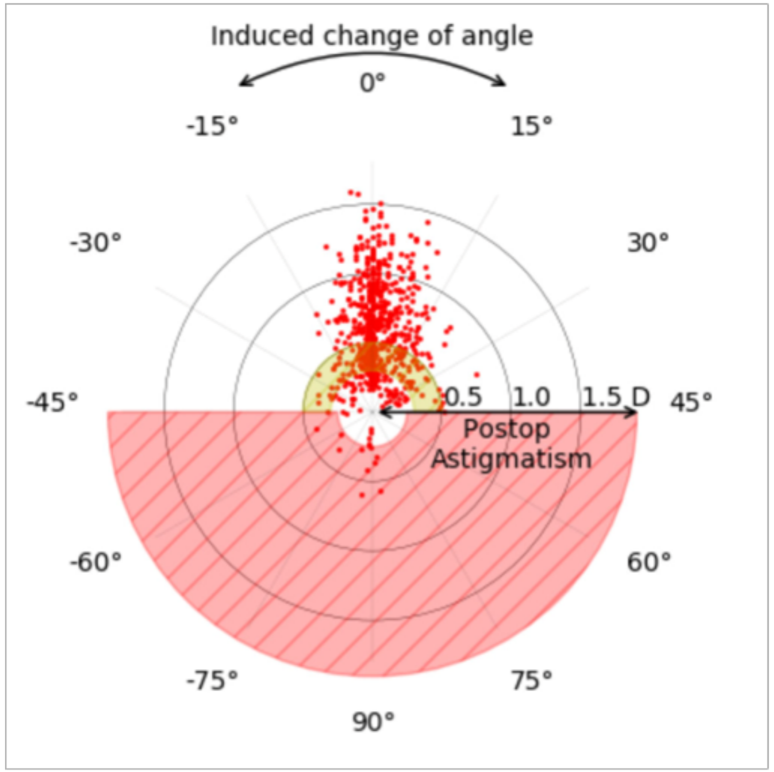

Donnenfeld nomogram

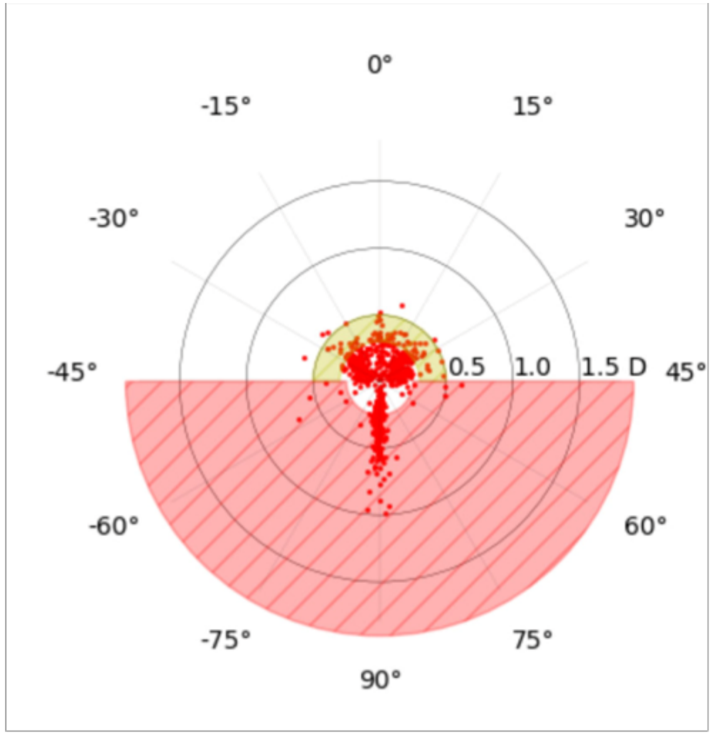

Lindström nomogram

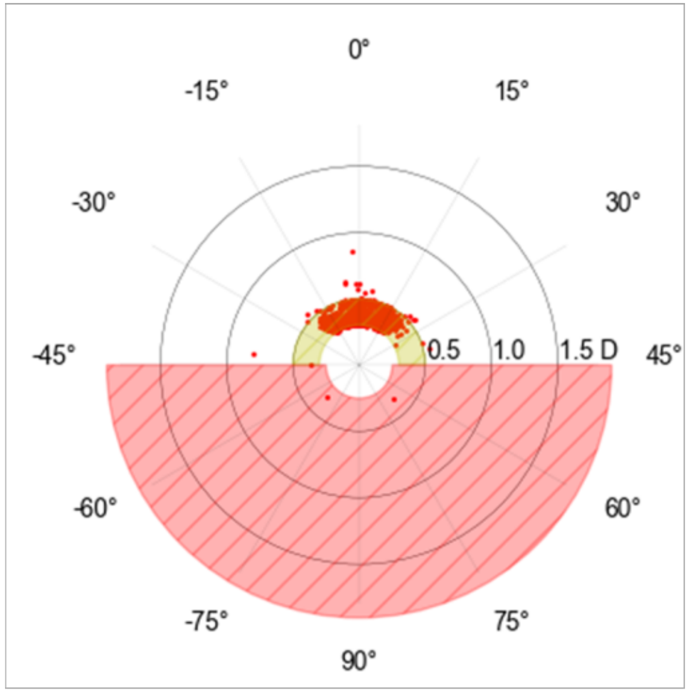

Optimization with target 0.4 D

Planning laser interventions

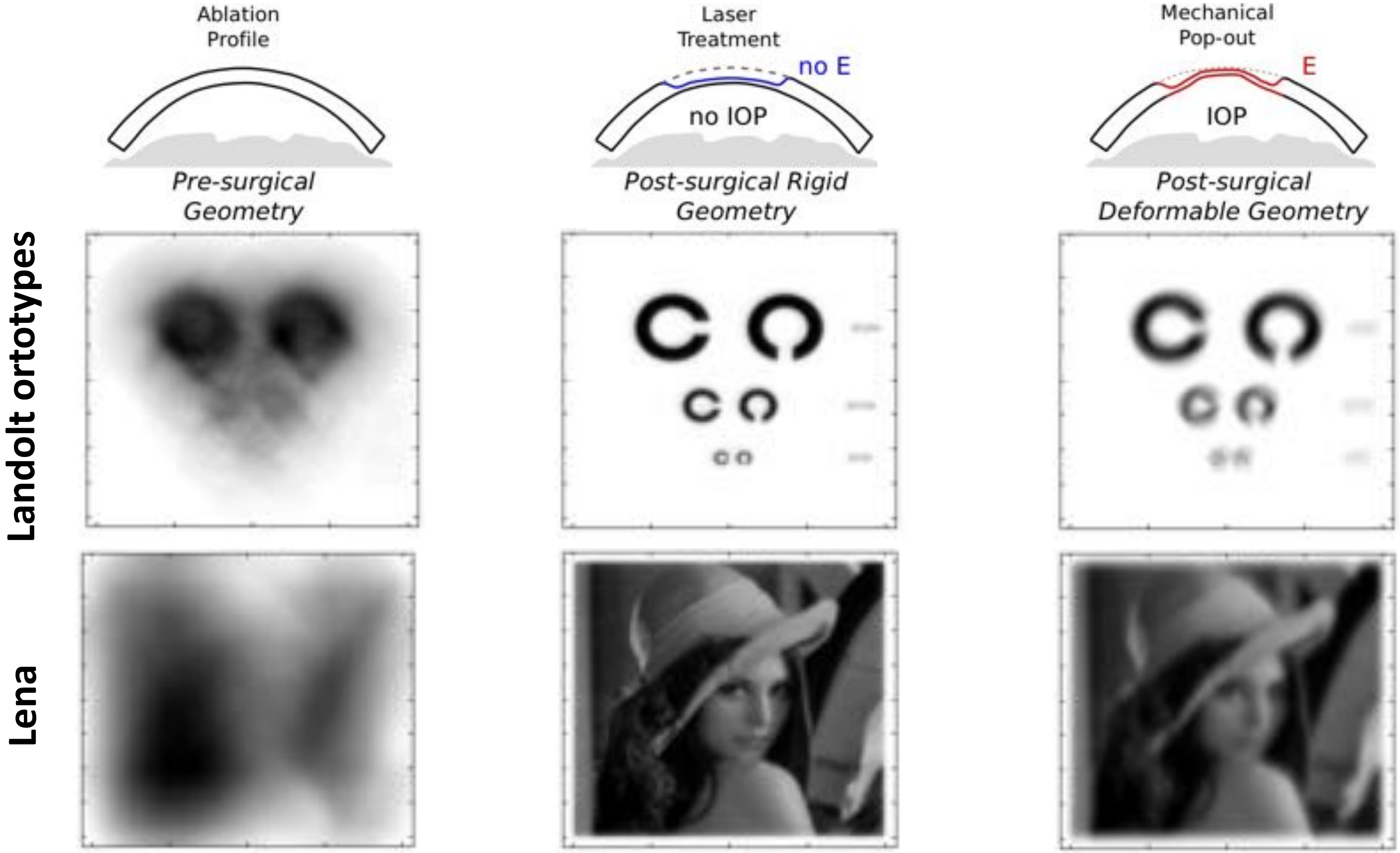

Summary

- Clinical planning based on FE simulations possible
  - Optimo-medical > 8 coworkers
  - Initial product for AK planning received CE mark
  - Partnerships with clinical centers
- Mechanical personalization remains challenging

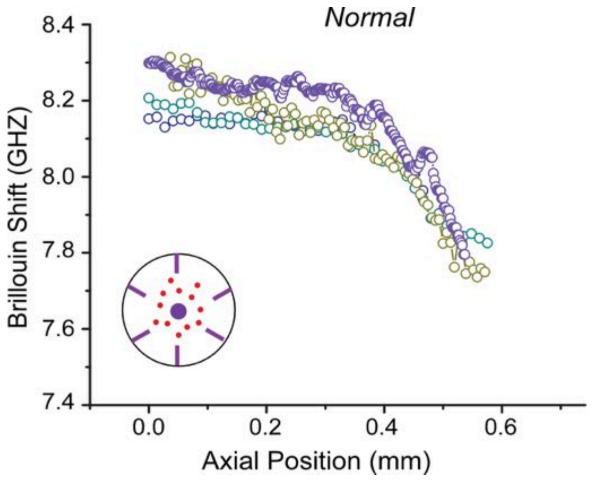

Brillouin microscopy

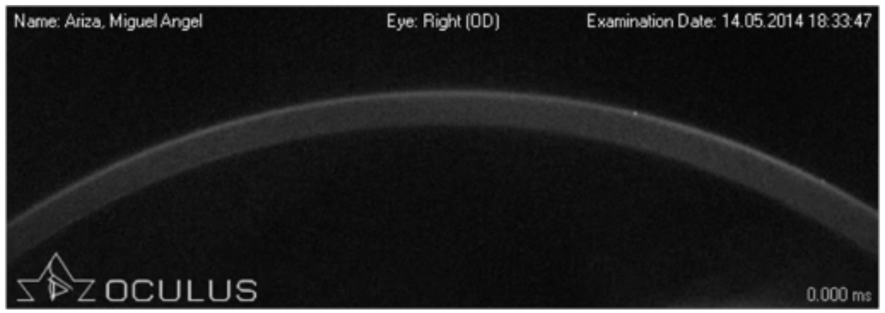

Non-contact tonometry

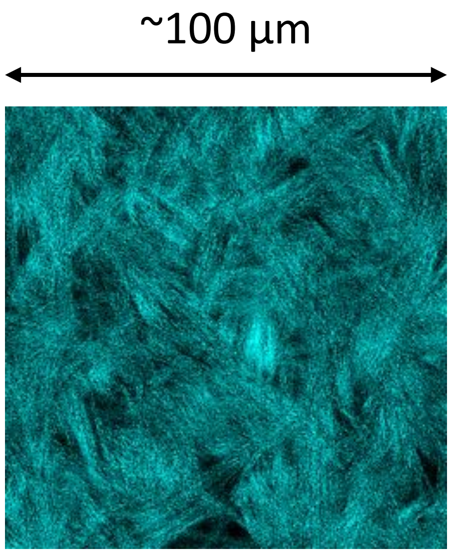

Tissue microstructure

UNIVERSITÄT BERN

Acknowledgements

Swiss National Science Foundation – Co-Me: Computer Aided and Image Guided Medical Interventions – Swiss Innovation Promotion Agency – EU Seventh Framework Programme – The ContraCancrum Project – Synthes AG – EU-CHIC – Swiss Heart Foundation – Universitätsspital Bern – Ozics Oy – Ansys, Inc – Stryker – PumpTire – Wissenschaftsfonds des Kantonsspitals Aarau – Integrated Scientific Services – Universitäts-Kinderspital beider Basel – Ziemer Group – Brainlab AG – Adoptics AG – Codman Neurosciences – Biovision AG – NanoTera.ch – Swiss Federal Institute of Technology – RegenHU – The Royal Academy of Engineering – Horizon 2020 – Marie Skłodowska-Curie Actions – OptimoMedical


Thank you
http://www.artorg.unibe.ch/